This article has been accepted for publication in a future issue of this journal, but has not been fully edited. Content may change prior to final publication. Citation information: DOI 10.1109/TAP.2021.3137405, IEEE Transactions on Antennas and Propagation

Postprint of: Pietrenko-Dąbrowska, A., & Koziel, S. (2022). Generalized Formulation of Response Features for Reliable Optimization of Antenna Input Characteristics. IEEE TRANSACTIONS ON ANTENNAS AND PROPAGATION, 70, 3733-3748. https://doi.org/10.1109/tap.2021.3137405

Generalized Formulation of Response Features for Reliable Optimization of Antenna Input Characteristics

Anna Pietrenko-Dabrowska, *Senior Member*, *IEEE*, Slawomir Koziel, *Senior Member*, *IEEE*

***Abstract*— Electromagnetic (EM)-driven parameter adjustment has become imperative in the design of modern antennas. It is necessary because the initial designs rendered through topology evolution, parameter sweeping, or theoretical models, are often of poor quality and need to be improved to satisfy stringent performance requirements. Given multiple objectives, constraints, and a typically large number of geometry parameters, the design closure should be carried out through numerical optimization. Unfortunately, standard algorithms entail high CPU expenses and are prone to failure. Feature-based optimization (FBO) is one of the methods developed to alleviate these difficulties by reformulating the design task in terms of the characteristic points extracted from EM-simulated responses. FBO capitalizes on a less nonlinear relationship between the feature point coordinates and antenna dimensions as compared to the original responses (e.g., frequency characteristics). This leads to flattening the functional landscape to be handled, faster convergence of the optimization algorithms, and a possibility of mitigating the issues pertinent to multi-modality. Notwithstanding, the response features have to be individually defined for each type of antenna response and tailored to a particular type of design specifications. This requires user experience and hinders a widespread application of FBO. This paper proposes a generalized and unified feature point definition, which is suitable for majority of typical antenna input characteristics (narrow-, multi-band, enhanced bandwidth, wideband), and performance specifications (matching improvement, bandwidth enhancement, mixture thereof). Our framework allows for an automated definition of the feature points given the performance specifications, along with their extraction from EM-simulated responses. The operation of the framework is illustrated using a range of planar antennas and favorably compared to conventional (non-feature-based) design closure task formulation.**

***Index Terms*— Antenna design; EM-driven design; parameter tuning; optimization; response features; computer-aided design.**

I. Introduction

Geometry parameter tuning through electromagnetic (EM)-driven optimization has nowadays become a commonplace in antenna design. It has various roots, among which the major role is played by a practical necessity. Beyond some elementary stand-alone structures (e.g., a simple patch antenna), it is virtually infeasible to arrive at the optimum set of dimensions using theoretical models or interactive parameter sweeping, especially when the antenna topology is complex and has to conform to multiple performance requirements pertinent to its electrical and field properties [1], [2]. Adequate accounting for variable interactions and their effects on antenna characteristics requires simultaneous adjustment of all parameters, which can only be achieved using numerical procedures [3]. To ensure design reliability at the presence of mutual coupling effects and environmental components (connectors, housing), antenna evaluation has to be carried out through EM analysis [4], [5]. EM-driven optimization may be computationally expensive even if only local (e.g., gradient-based [6]) search is needed. Global optimization [7]-[11], required in the case of poor initial design or multi-modality [12] of the objective function, entails considerably higher expenses. The cost of other simulation-based tasks such as uncertainty quantification (statistical analysis [13], yield optimization [14]) or multi-objective design [15], [16], may be unmanageable when conducted using conventional techniques, unless the objective function is fast to evaluate (e.g., involves analytical array factor models) [17]-[19]. It should also be mentioned that certain factors, including a potentially high dimensionality of the parameter space (typical for modern antenna systems), considerably aggravate these challenges. The continuous advancements in simulation software and computing hardware mitigate the problem but only to some extent, because the increasing complexity of the antenna topologies, the need for including in the analysis previously neglected effects (e.g., substrate anisotropy [20], the presence of neighboring devices [21], etc.), act in the opposite direction and prolong the simulation times.

The research efforts undertaken to address the aforementioned difficulties led to the development of a variety of techniques that aim at making EM-driven design procedures faster and more reliable. In the realm of gradient-based algorithms [22], a notable example is the incorporation of adjoint sensitivities [23], [24], which is, however, an intrusive technique of limited accessibility through commercial simulation packages [25]. Non-intrusive methods include the algorithms with sparse sensitivity updates [26], typically based

The manuscript was submitted on March 15, 2021. This work was supported in part by the Icelandic Centre for Research (RANNIS) Grant 217771, and by Gdańsk University of Technology Grant DEC-41/2020/IDUB/I.3.3 under the Argentum Triggering Research Grants program - 'Excellence Initiative - Research University'.

S. Koziel is with Engineering Optimization and Modeling Center of Reykjavik University, Reykjavik, Iceland (e-mail: koziel@ru.is); A. Pietrenko-Dabrowska and also S. Koziel are with Faculty of Electronics, Telecommunications and Informatics, Gdansk University of Technology, 80-233 Gdansk, Poland.

This article has been accepted for publication in a future issue of this journal, but has not been fully edited. Content may change prior to final publication. Citation information: DOI 10.1109/TAP.2021.3137405, IEEE Transactions on Antennas and Propagation

on detecting the stability patterns for antenna response Jacobians [27] or employing selectively applied updating formulas [28]. Another group of techniques is those exploring variable-fidelity models, which, in the case of antennas, are mostly based on variable-resolution EM simulations [29]. The main idea is to shift the computational burden onto the lower-fidelity representation, often in the form of a physics-based surrogate, with only occasional reference to the high-fidelity EM analysis (for design verification and surrogate model enhancement). Popular implementations include space mapping [30] (with its various implementations [31]-[33]), as well as response correction techniques (e.g., manifold mapping [34], adaptive response scaling [35], shape-preserving response prediction [36]). Surrogate-assisted approaches involving data-driven models [37]-[42] have been drawing more and more attention over the recent years due to their versatility. These methods often interleave the surrogate model construction and the prediction stage (local or global optimization) through sequential design of experiments involving various infill criteria, e.g., maximization of expected improvement or minimization of the statistical lower bound [43]. Among the techniques of this group that are popular in antenna design kriging [44], radial basis functions [45], or neural networks [46] may be listed. Recently, integration of global optimization with machine learning has been fostered as a way of efficient handling of multidimensional parameter spaces [66-70].

The methods mentioned in the previous paragraph are conventional in the sense of the design problem formulation, in particular, they operate on the original system outputs (e.g., the frequency characteristics), and use appropriately defined merit functions defined over these outputs. On the other hand, response features methodologies [47], [48] attempt to exploit a particular structure of the system outputs as well as the fact that the dependence of the frequency and level coordinates of suitably-defined characteristic points of these responses exhibit less nonlinear dependence on the design parameters than the original ones, when considered in their entirety [47]. Reformulation of the design task (e.g., parametric optimization) in terms of response features leads to flattening the objective function landscape and allows for improving the reliability and the computational efficiency of the EM-driven procedures [47], [49]. In some cases, e.g., microwave devices such as filters, the response features may be selected as zeros and poles of the transfer function [50], or the entries of the coupling matrix [51]. However, the most generic approach (e.g., [47]), more suitable for antennas, assumes that the characteristics points are defined on and directly extracted from the simulated frequency characteristics of the system under design. These may be the location of the antenna resonances [47], the minima of the coupler matching/isolation responses [52], the local (in-band) maxima of the filter return loss characteristic [53], [54], or the points corresponding to particular response levels (e.g., –10 dB when determining the antenna impedance bandwidth) [47]. In other words, the feature definition depends on the design problem (i.e., considered performance figures and requirements), and the type of response (narrow-band, multi-band, broadband, etc.). Both make the technique less accessible for inexperienced users.

This paper proposes a generalized formulation of the response feature technology for optimization of antenna input characteristics. In particular, we discuss a unified definition of the feature points, which is suitable for the majority of antenna responses, including the narrow-band, multi-band, enhanced-bandwidth, and broadband responses. Furthermore, our approach enables handling of various types of performance requirements (matching improvement, bandwidth enhancement), allows for automated definition of the feature points given the specifications, as well as their extraction from EM-simulated responses. The numerical results obtained for several antenna structures of different input characteristics corroborate versatility of the approach and the computational benefits it provides when compared to the standard (non-feature-based) formulation of the design closure problem. It should be emphasized that the scope of this paper is limited to input characteristics. Generalization for other types of responses (gain, axial ratio, etc.) will be addressed in the future work.

The novelty and the technical contributions of this work include: (i) a unified definition of the feature points suitable for the majority of antenna input characteristics and handling of various types of performance requirements, (ii) a conceptual development of the optimization framework using the generalized formulation of the response feature technology for optimization of antenna input characteristics, (iii) implementation of the generalized feature-based optimization algorithm integrating local gradient-based search with automated response feature definition, (iv) comprehensive verification of suitability of the proposed generalized feature-based optimization approach for rendering optimal designs satisfying the assumed performance requirements. The verification is based on four antenna structures of distinct response types and different formulations of the design task. To the best knowledge of the authors, this is the first exposition of a versatile feature-based optimization framework proposed in the literature that does not require individual definition of the characteristics points by the user, and allows for capitalizing on all of the benefits of this technology for antenna parameter tuning. At the same time, it should be emphasized that the considered methodology is a customized approach capitalizing on the ability to define and explore the characteristic points of antenna responses. Consequently, it is not a general-purpose optimization technique, yet its versatility is greatly improved over the previously reported variations of the response-feature-based optimization frameworks.

II. Response Features. Generalized Feature-Based Optimization

This section introduces the concept of generalized feature-based optimization, here, considered for antenna input characteristics. Handling of other types of responses, such as gain or axial ratio, will be addressed elsewhere. The section begins by formulating the antenna design closure task (Section II.*A*). Conventional feature-based optimization and its benefits but also limitations are discussed in Section II.*B*. Sections II.*C* through II.*E* introduce generalized response features. A unified

This article has been accepted for publication in a future issue of this journal, but has not been fully edited. Content may change prior to final publication. Citation information: DOI 10.1109/TAP.2021.3137405, IEEE Transactions on Antennas and Propagation

definition of characteristics points suitable for various types of antenna input characteristics (multi-band, wideband, etc.) is outlined in Section II.*C*. Feature-based objective function definition is dealt with in Section II.*D*. Section II.*E* discusses the overall algorithm operation and illustrates it using a flow diagram.

A. Antenna Design Closure: Problem Formulation

The primary computational representation of the antenna under design is a full-wave EM model $\boldsymbol{R}(\boldsymbol{x})$ that returns all relevant characteristics (reflection $S_{11}(\boldsymbol{x})$, gain $G(\boldsymbol{x})$, etc.). It is a function of a designable variable vector $\boldsymbol{x}$ that contains all independent (mostly geometry) parameters undergoing the adjustment process. In the numerical optimization nomenclature, the design closure task can be formulated as

$$\boldsymbol{x}^* = \arg\min_{\boldsymbol{x}} U(\boldsymbol{R}(\boldsymbol{x})) \tag{1}$$

where $\boldsymbol{x}^*$ is the optimum design to be identified, whereas U is the objective function that encodes the design requirements imposed upon the structure. Often, the objective function is of a minimax type, i.e., a set of lower and/or upper acceptance levels is defined over the specified frequencies or frequency bands. For example, when optimizing a wideband antenna to improve its matching over the frequency range $f \in [f_L, f_U]$, the function U would be defined as

$$U(\boldsymbol{R}(\boldsymbol{x})) = \max\{f_L \le f \le f_U : |S_{11}(\boldsymbol{x}, f)|\} \tag{2}$$

If the antenna is optimized to reduce the gain variation over the same frequency range while satisfying the condition $|S_{11}(\boldsymbol{x},f)| \le -10$ dB for $f_L \le f \le f_R$, the objective function could be defined as

$$\begin{aligned} U(\boldsymbol{R}(\boldsymbol{x})) = {} & \max\{f_L \le f \le f_R : G(\boldsymbol{x})\} + \\ & -\min\{f_L \le f \le f_R : G(\boldsymbol{x})\} + \beta c(\boldsymbol{x})^2 \end{aligned} \tag{3}$$

where $c(\boldsymbol{x}) = \max\{\max\{f_L \le f \le f_R : |S_{11}(\boldsymbol{x},f)| + 10\},0\}$ is a penalty function enforcing the matching condition. The latter may be also handled explicitly, as a design constraint. Similarly, optimizing a multi-band antenna to be matched at the target operating frequencies $f_{0,j}$, $j = 1, ..., N$, would imply the following function U:

$$U(\boldsymbol{R}(\boldsymbol{x})) = \max\{|S_{11}(\boldsymbol{x}, f_{0.1})|,...,|S_{11}(\boldsymbol{x}, f_{0.N})|\} \tag{4}$$

The particular cases mentioned above constitute merely selected examples that are supposed to give a flavor of a large variety of possible options. Other design scenarios will be discussed later in the paper.

B. Feature-Based Optimization: Formulation, Benefits, and Challenges

Feature-based optimization (FBO) has been introduced in [47] as a way of improving computational efficiency and reliability of EM-driven design procedures. FBO departs from the original formulation of the design problem (cf. Section II.*A*) and expresses the performance requirements in terms of appropriately defined characteristic points of the antenna responses. For the sake of further discussion, we denote the feature points as $\boldsymbol{p}_k = [f_k\ l_k]$, $k = 1, \ldots, N_p$, where f_k and l_k stand for the frequency and level coordinate of the kth point, and N_p is the number of features defined for a given antenna structure. The aggregated feature vector will be denoted as $\boldsymbol{P}(\boldsymbol{x}) = [\boldsymbol{p}_1(\boldsymbol{x}) \ldots \boldsymbol{p}_{Np}(\boldsymbol{x})]^T$. FBO capitalizes on the fact that the dependence between the design parameters $\boldsymbol{x}$ and the coordinates f_k and l_k is significantly less nonlinear than a similar dependence for the original responses, i.e., $\boldsymbol{R}(\boldsymbol{x})$ [47], as illustrated in Fig. 1 for a dual-band antenna with the feature points being the locations of the antenna resonances. The following consequences of the aforementioned property can be observed:

- Reformulating the original design problem (1) in terms of the feature points results in "flattening" the functional landscape to be handled by the optimization algorithm, which leads to improved reliability and a faster convergence [47];
- When used in the modelling context, feature-based approach may enable considerable computational savings in terms of training data acquisition, i.e., less training samples are required (as compared to operating at the level of frequency characteristics) to render the surrogates of similar predictive power [48];
- Operating at the level of response features facilitates frequency manipulation of the antenna characteristics (e.g., shifting the resonances to different operating frequencies), which is usually challenging when handling the entire responses through, e.g., minimax objective functions;
- Using response features often allows us to get away with poor initial designs, in particular, the use of local search procedures may be sufficient even in situations normally requiring global algorithms [49].

The advantages of FBO (and response feature approach in general) have been demonstrated in the context of design optimization of multi-band [48] and broadband antennas [55], microwave couplers [52], surrogate modeling [48], uncertainty quantification [54], as well as globalized search [49].

Selection of the feature points is generally problem dependent. It might be related to the circuit transfer function (e.g., pole and zero location) [50], or may be directly extracted from the circuit responses (e.g., locations of the resonances [47] or local maxima of the filter return loss characteristic in the passband [53]). In either case, the prerequisite is that the information carried by the characteristic points is sufficient to account for the design specifications. For illustration, let us consider the minimax objective function (4) of Section II.*A*, defined for the problem of allocating the antenna resonances at the target operating frequencies $f_{0,j}$, $j = 1, \ldots, N$, and improving the matching therein. In this case, it is sufficient to select the response features to be the locations of the antenna resonances so that we have $\boldsymbol{p}_k(\boldsymbol{x}) = [f_{r.k}(\boldsymbol{x})\ l_{r.k}(\boldsymbol{x})]$, $k = 1, \ldots, N$, where $f_{r.k}(\boldsymbol{x})$ and $l_{r.k}(\boldsymbol{x})$ are the resonant frequencies and the corresponding reflection levels. Using these, the feature-based objective function U_F can be defined as

$$\begin{aligned} U_F(\boldsymbol{P}(\boldsymbol{x})) = {} & \max\{l_{r.1}(\boldsymbol{x}),...,l_{r.N}(\boldsymbol{x})\} + \\ & + \beta \left\| \begin{bmatrix} f_{0.1} \\ \vdots \\ f_{0.N} \end{bmatrix} - \begin{bmatrix} f_{r.1}(\boldsymbol{x}) \\ \vdots \\ f_{r.2}(\boldsymbol{x}) \end{bmatrix} \right\|^2 \end{aligned} \tag{5}$$

where β is a multiplication factor determining the contribution of the frequency misalignment term into the objective function.

This article has been accepted for publication in a future issue of this journal, but has not been fully edited. Content may change prior to final publication. Citation information: DOI 10.1109/TAP.2021.3137405, IEEE Transactions on Antennas and Propagation

It should be noted that the optimum designs according to (4) and (5) coincide (assuming that it is possible to perfectly match the target frequencies), yet the profile of (5) along the line section considered in Fig. 1 is monotonic as opposed to that of (4), cf. Fig. 2, which makes the problem easier to handle.

As mentioned before, the response features need to be defined so that the information therein allows us to account for performance specifications imposed on the system at hand. This is illustrated in Fig. 3, where—for the purpose of matching improvement at the target frequency—the right choice of the feature point would be the location of the resonance, whereas for the sake of bandwidth enhancement, it is more appropriate to select the points corresponding to –10 dB levels of the reflection characteristic.

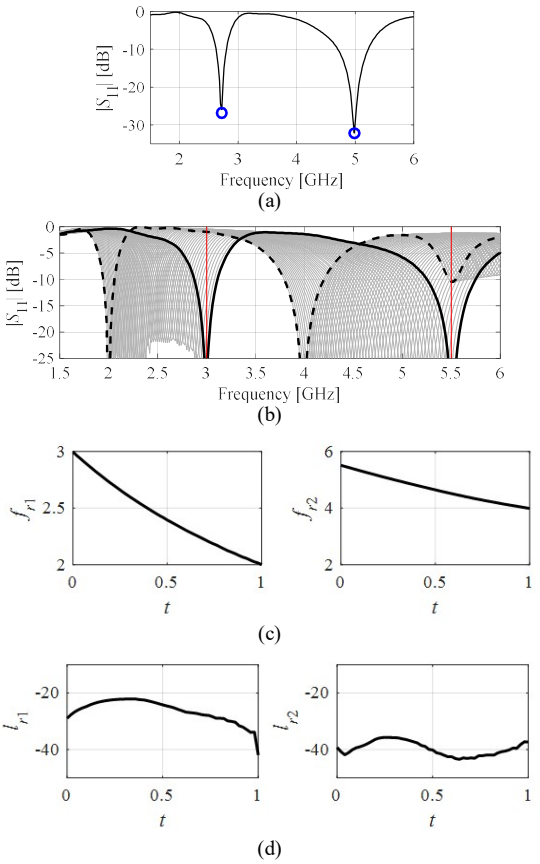

Fig. 1. Response feature concept: (a) example reflection characteristic of a dual band antenna and the feature points corresponding to the antenna resonances (o); (b) exemplary initial design (- - -), the design optimized for target frequencies 3.0 GHz and 5.5 GHz (—), and the family of reflection responses along the line segment connecting these two designs, parameterized by $0 \le t \le 1$ (gray lines); (c) feature point coordinates as functions of the parameter t.

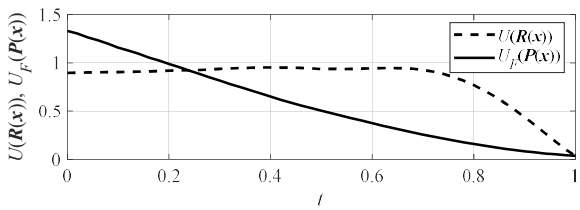

Fig. 2. Minimax objective function (4) (- - -) and feature-based objective function (5) (—) versus parameter t (cf. Fig. 1). The feature-based objective function is smoother, monotonic, and the target design is reachable from the given initial point through local search.

C. Generalized Response Features: Feature Point Definition

In general, the feature definition, its extraction from EM-simulated antenna responses as well as a definition of the feature-based objective function has to be tailored to a particular type of antenna response and a specific design task. This is perhaps the most serious disadvantage of the FBO technique in terms of its automation because the setup of the optimization framework requires a certain amount of user experience and interaction. This work proposes a unified definition of response features so that the characteristic points can be defined and extracted automatically regardless of a specific set of performance specifications, and subsequently used to formulate a feature-based objective function (which will be dealt with in Section II.*D*). As mentioned in the introduction, in this paper, our considerations are restricted to antenna input characteristics (reflection response). Generalization to other types of responses such as gain or axial ratio will be given elsewhere.

Design specifications concerning the antenna reflection response are either related to matching improvement (or satisfying given acceptance thresholds) at a specific frequency band (or bands in the case of multi-band structures), or to bandwidth enhancement at, and in the vicinity of the specific operating frequencies. Thus, when considering the characteristic points capable of accounting for the aforementioned types of requirements, one needs to include the following:

- A point corresponding to the reflection minimum within the bandwidth; the left-most local minimum is to be considered;
- Bandwidth-defining points, which for the reflection characteristic would be those corresponding to –10 dB level of $|S_{11}|$;
- Points corresponding to the target operating frequencies;
- Points corresponding to the levels in the middle (in dB scale) between the reflection minimum and 0 dB;
- Points corresponding to the local maxima within the bandwidth.

The rationale behind selecting these particular points will be elaborated on further in this section. The above set of points will be considered the maximum feature set, which may be reduced for some cases by merging the points that belong to different categories, depending on the type of antenna response, the design specifications, or simply the fact that some of the points may be non-existent at particular designs. Furthermore, in the case of multi-band antennas, there will be a separate set of feature points corresponding to each band. However, for the sake of simplifying the discussion, we assume the case of a single-band antenna at the moment. Figure 4 illustrates the definition and the meaning of the particular categories of feature points. In the exemplary situation shown in the picture, all types of points are present. Notwithstanding, in many practical situations, one will often encounter degenerate cases. These will be discussed later in the section.

The following notation will be used throughout (for the sake of brevity, henceforth, the dependence of the entries of the vector $\boldsymbol{P}(\boldsymbol{x})$ on the design variables will be omitted)

This article has been accepted for publication in a future issue of this journal, but has not been fully edited. Content may change prior to final publication. Citation information: DOI 10.1109/TAP.2021.3137405, IEEE Transactions on Antennas and Propagation

$$\boldsymbol{P}(\boldsymbol{x}) = [\boldsymbol{p}_{\min}\ \boldsymbol{p}_{-10.L}\ \boldsymbol{p}_{-10.R}\ \boldsymbol{p}_L\ \boldsymbol{p}_R\ \boldsymbol{p}_{L/2}\ \boldsymbol{p}_{R/2}\ \boldsymbol{p}_{\max.1}\ \cdots] \quad (6)$$

where (f and l stand for the frequency and the level coordinates of the feature points):

- $\boldsymbol{p}_{\min} = [f_{\min}\ l_{\min}]^T$ – feature point corresponding to the left-most in-band minimum;
- $\boldsymbol{p}_{-10.L} = [f_{-10.L}\ l_{-10.L}]^T$, $\boldsymbol{p}_{-10.R} = [f_{-10.R}\ l_{-10.R}]^T$ – feature points corresponding to –10 dB reflection levels (left- and right-hand side, respectively);
- $\boldsymbol{p}_L = [f_L\ l_L]^T$, $\boldsymbol{p}_R = [f_R\ l_R]^T$ – feature points corresponding to the target bandwidth frequencies f_L and f_H, respectively;
- $\boldsymbol{p}_{L/2} = [f_{L/2}\ l_{L/2}]^T$, $\boldsymbol{p}_{R/2} = [f_{R/2}\ l_{R/2}]^T$ – feature points corresponding to the level in the middle (in dB scale) between the reflection minimum and 0 dB;
- $\boldsymbol{p}_{\max.k} = [f_{\max.k}\ l_{\max.k}]^T$ – feature points corresponding to the kth local in-band reflection maximum. For the purpose of extracting $\boldsymbol{p}_{\max.k}$, the bandwidth is understood as the frequency range between $\min\{f_{-10.L}, f_{L/2}\}$ and $\max\{f_{-10.R}, f_{R/2}\}$.

The reason for defining these particular types of points is that they are necessary but also sufficient to account for the various types of performance specifications that one may encounter while handling the reflection characteristics of antennas. In particular:

- $\boldsymbol{p}_{\min}$ can be used to control the antenna matching at the operating frequency (in the cases of narrow- and multi-band antennas) as well as to relocate the antenna resonances towards the target frequencies.
- $\boldsymbol{p}_{-10.L}$ and $\boldsymbol{p}_{-10.R}$ can be used to control the antenna bandwidth (e.g., when optimizing the antenna for maximum bandwidth);
- $\boldsymbol{p}_L$ and $\boldsymbol{p}_R$ will be useful to implement minimax type of specifications (e.g., matching improvement over a specific frequency range);
- $\boldsymbol{p}_{L/2}$ and $\boldsymbol{p}_{R/2}$ are auxiliary points that will be useful to approximately determine antenna bandwidth in some degenerate cases (e.g., when the overall in-band reflection level is above –10 dB);
- $\boldsymbol{p}_{\max.k}$ will be employed to control antenna matching for minimax type of specifications (e.g., in the cases of wideband structures);

As mentioned before, some of the features may or may not exist for a given instance of the reflection characteristic:

- If the minimum reflection level in the vicinity of the antenna operating bandwidth is higher than –10 dB, neither $\boldsymbol{p}_{-10.L}$ nor $\boldsymbol{p}_{-10.R}$ exist and we assign $\boldsymbol{p}_{-10.L} = \boldsymbol{p}_{-10.R} = \boldsymbol{p}_{\min}$;
- If the reflection characteristic does not have any local maxima in the operating band, the points $\boldsymbol{p}_{\max.k}$ are not assigned;
- In some cases, one may have $f_L = f_R = f_0$, i.e., the design specifications are defined with respect to an operating frequency f_0 rather than the operating bandwidth $[f_L\ f_R]$. In this situation, we assign $\boldsymbol{p}_L = \boldsymbol{p}_R = \boldsymbol{p}_0 = [f_0\ l_0]^T$, where l_0 is the response level at f_0.

The reason for the above assignments is that for the sake of practical handling of the response features (e.g., through numerical procedures), it is more convenient to maintain a constant number of points (apart from the local maxima, which are at the end of the response feature vector), so that their identification within $\boldsymbol{P}(\boldsymbol{x})$ is straightforward. Figure 5 shows several degenerate situations that may be encountered in practice. Depending on the case, some of the points may not be defined as described above.

It should also be noted that some of the feature points may not be well-defined simply because of a limited frequency range of antenna simulation. This would be typically the case for ultra-wideband antennas which are well matched even for the highest simulation frequency. Therein, the feature points $\boldsymbol{p}_R$ and $\boldsymbol{p}_{R/2}$ may not exists.

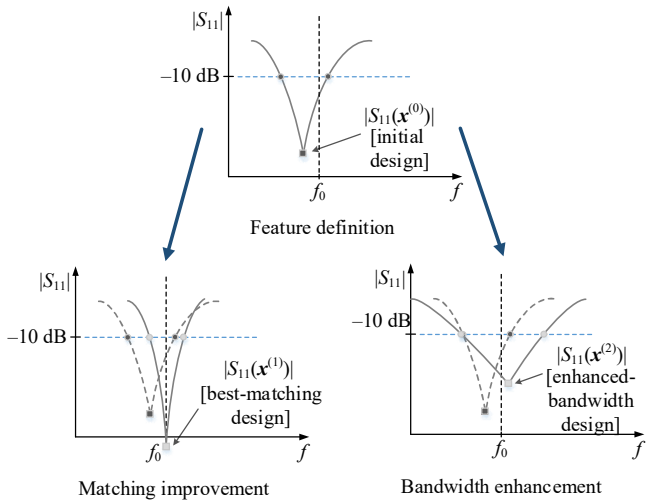

Fig. 3. Selecting response features for particular design tasks. The feature point corresponding to the antenna resonance can be used for matching improvement at the target frequency f_0 (left plot). The points corresponding to –10 dB levels can be employed for bandwidth enhancement (right plot).

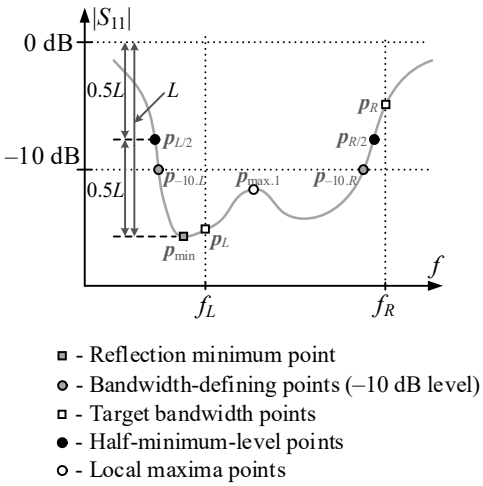

Fig. 4. Example reflection response, target bandwidth (frequencies f_L and f_R), and the feature points: $\boldsymbol{p}_{\min}$ – the left-most local reflection minimum; $\boldsymbol{p}_{-10.L}$, $\boldsymbol{p}_{-10.H}$ – the points corresponding to –10 dB levels; $\boldsymbol{p}_L$, $\boldsymbol{p}_H$ – the points corresponding to the target frequencies f_L and f_H; as well as $\boldsymbol{p}_{L/2}$, $\boldsymbol{p}_{H/2}$ – the points corresponding to the levels determined by half of the distance between 0 dB and the level of the minimum point (in dB), and the local maxima ($\boldsymbol{p}_{\max.k}$). In this case, the characteristic only contains one in-band local maximum (i.e., $k = 1$). The picture shows a generic situation where all types of feature points actually exist. Degenerate situations will be discussed later in the section, see also Fig. 5.

This article has been accepted for publication in a future issue of this journal, but has not been fully edited. Content may change prior to final publication. Citation information: DOI 10.1109/TAP.2021.3137405, IEEE Transactions on Antennas and Propagation

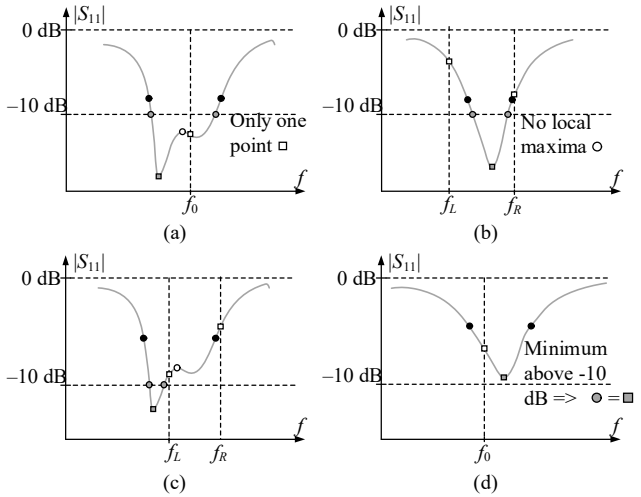

Fig. 5. Response features for several specific scenarios (explanations of the feature points can be found in Fig. 4): (a) the presence of a single operating frequency f_0 (instead of the target bandwidth defined by the frequencies f_L and f_R), (b) the lack of local maxima, (c) part of the operating bandwidth below –10 dB, in which case half-level points are more appropriate to estimate the antenna bandwidth than –10 dB ones, (d) reflection minimum above –10 dB, in which case the–10 dB points are assigned to be identical to the minimum point.

In the case of multi-band antenna, each band will have an independent set of feature points extracted according to the same rules as discussed in this section. The overall feature point structure will consist of vectors

$$\boldsymbol{P}_j(\boldsymbol{x}) = [\boldsymbol{p}_{j.\min}\ \boldsymbol{p}_{j.-10.L}\ \boldsymbol{p}_{j.-10.R}\ \boldsymbol{p}_{j.L}\ \boldsymbol{p}_{j.R}\ \boldsymbol{p}_{j.L/2}\ \boldsymbol{p}_{j.R/2}\ \boldsymbol{p}_{j.\max.1}\ \ldots] \quad (7)$$

with $j = 1, \ldots, N_B$, where N_B is the number of antenna operating bands.

D. Generalized Response Features: Objective Function Definition

The primary purpose of the feature-based technology is to improve the reliability and to expedite the design optimization procedures. Having a unified definition of response features, our next goal is to develop a versatile formulation of the feature-based objective function that would express the original (often, minimax) objectives imposed on the antenna reflection characteristic in terms of the feature point coordinates. To this end, we will consider several types of specifications, which essentially cover most of the practical possibilities in terms of antenna reflection response manipulation, the designer might want to pursue. For the sake of notational simplicity, the list below concerns single-band antennas but generalization for multi-band cases is straightforward. Similarly as before, f_0 will be referred to as a (single) target frequency, whereas f_L and f_R will denote the target operating bandwidth:

- Matching improvement within the frequency range $[f_L\ f_R]$ (which implies relocation of the antenna operating bandwidth near $[f_L f_R]$).
- Matching improvement at f_0 (which implies relocation of the antenna resonance to f_0);
- Maximization of bandwidth that includes the frequency range $[f_L f_R]$ (relocation of the antenna operating bandwidth near $[f_L f_R]$ is implied).
- Maximization of (symmetric) bandwidth around the center frequency f_0 (relocation of antenna operating bandwidth towards f_0 is implied);

However, as mentioned before, the second and the fourth case are special cases of the first and the third one, respectively (with the assignment of $f_L = f_R = f_0$, and $\boldsymbol{p}_L = \boldsymbol{p}_R = \boldsymbol{p}_0 = [f_0\ l_0]^T$). Thus, in the following, only these two cases (matching improvement and bandwidth maximization) will be considered.

1) Feature-Based Objective Function for In-band Matching Improvement

The objective function for matching improvement will be defined as (single-band case)

$$U_F(\boldsymbol{P}(\boldsymbol{x})) = \max\{l_L(\boldsymbol{x}), l_R(\boldsymbol{x}), l_{\max.1}(\boldsymbol{x}), \ldots\} + \beta_m\left[c_{m.L}(\boldsymbol{x})^2 + c_{m.R}(\boldsymbol{x})^2\right] \quad (8)$$

where

$$c_{m.L}(\boldsymbol{x}) = \max\{\min\{f_{-10.L}(\boldsymbol{x}), f_{L/2}(\boldsymbol{x})\} - f_L, 0\} \quad (9)$$

$$c_{m.R}(\boldsymbol{x}) = \max\{f_R - \min\{f_{-10.R}(\boldsymbol{x}), f_{R/2}(\boldsymbol{x})\}, 0\} \quad (10)$$

The first term in (8), which is the primary objective, represents the maximum in-band reflection to be minimized. Note that for the case $f_L = f_R = f_0$ (single operating frequency instead of a range $[f_L f_R]$), this term reduces to $l_0(\boldsymbol{x})$. The second term is a penalty factor that allows us to relocate the antenna bandwidth to $[f_L f_R]$. The penalty term has a non-zero contribution if either the left-hand-side edge of the actual operating band is higher than the target f_L, or the right-hand-side edge of the operating band is lower than the target f_R.

Generalization of (8)-(10) for the case of multi-band antennas will take the form of

$$U_F(\boldsymbol{P}(\boldsymbol{x})) = \max\{l_{1.L}(\boldsymbol{x}), \ldots, l_{N_B.L}(\boldsymbol{x}), l_{1.R}(\boldsymbol{x}), \ldots l_{N_B.R}(\boldsymbol{x}), l_{1.\max.1}(\boldsymbol{x}), \ldots, l_{N_B.\max.1}(\boldsymbol{x}), \ldots\} + \beta_m\left[\sum_{j=1}^{N_B} c_{j.m.L}(\boldsymbol{x})^2 + \sum_{j=1}^{N_B} c_{j.m.R}(\boldsymbol{x})^2\right] \quad (11)$$

with

$$c_{j.m.L}(\boldsymbol{x}) = \max\{\min\{f_{j.-10.L}(\boldsymbol{x}), f_{j.L/2}(\boldsymbol{x})\} - f_{j.L}, 0\} \quad (12)$$

$$c_{j.m.R}(\boldsymbol{x}) = \max\{f_{j.R} - \min\{f_{j.-10.R}(\boldsymbol{x}), f_{j.R/2}(\boldsymbol{x})\}, 0\} \quad (13)$$

The above definitions are consistent with the "traditional" feature-based objective functions. For example, it can be observed that the objective function (5) considered in Section II.*B* is a special case of (11)-(13) because we have: $l_{j.L}(\boldsymbol{x}) = l_{j.R}(\boldsymbol{x}) = l_{j.\min}(\boldsymbol{x}) = l_{r.j}$ for $j = 1, \ldots, N_B = N$, i.e., the first term in (11) becomes $\max\{l_{r.1}(\boldsymbol{x}), \ldots, l_{r.N}(\boldsymbol{x})\}$. Also, $f_{j.-10.L}(\boldsymbol{x}) = f_{j.-10.R}(\boldsymbol{x}) = f_{j.\min}(\boldsymbol{x}) = f_{r.j}$, hence $f_{j.L/2}(\boldsymbol{x}) < f_{j.-10.L}(\boldsymbol{x})$ and $f_{j.R/2}(\boldsymbol{x}) > f_{j.-10.R}(\boldsymbol{x})$. Due to these relations we have $\min\{f_{j.-10.L}(\boldsymbol{x}), f_{j.L/2}(\boldsymbol{x})\} - f_{j.L}\} = f_{j.L/2}(\boldsymbol{x}) - f_{0.j}$ and $f_{j.R} - \min\{f_{j.-10.R}(\boldsymbol{x}), f_{j.R/2}(\boldsymbol{x})\} = f_{0.j} - f_{j.R/2}(\boldsymbol{x})$. Now, if $f_{j.L/2}(\boldsymbol{x}) < f_{0.j}$ then $c_{j.m.L}(\boldsymbol{x}) = 0$, otherwise, $c_{j.m.L}(\boldsymbol{x}) = f_{j.L/2}(\boldsymbol{x}) - f_{0.j}$. Similarly, if $f_{0.j} < f_{j.R/2}(\boldsymbol{x})$ then $c_{j.m.R}(\boldsymbol{x}) = 0$, otherwise

This article has been accepted for publication in a future issue of this journal, but has not been fully edited. Content may change prior to final publication. Citation information: DOI 10.1109/TAP.2021.3137405, IEEE Transactions on Antennas and Propagation

$c_{j.m.R}(\boldsymbol{x}) = f_{0.j} - f_{j.R/2}(\boldsymbol{x})$. Thus, the second term in (11) becomes

$$\begin{aligned}&\sum_{j=1}^{N_B} c_{j.m.L}(\boldsymbol{x})^2 + \sum_{j=1}^{N_B} c_{j.m.R}(\boldsymbol{x})^2 = \\ &= \sum_{j=1}^{N_B} (\max\{f_{j.L/2}(\boldsymbol{x}) - f_{0.j}, 0\})^2 + \\ &+ \sum_{j=1}^{N_B} (\min\{f_{j.R/2}(\boldsymbol{x}) - f_{0.j}, 0\})^2\end{aligned} \tag{14}$$

The term (14) becomes zero if the antenna operating frequencies are sufficiently close to the target frequencies, i.e., $f_{j.L/2} < f_{0.j} < f_{j.R/2}$ for all j, and it is proportional to the second power of the respective frequency differences otherwise. On the other hand, the penalty term in (5) gets close to zero under the same conditions, i.e., $f_{r.j} \approx f_{0.j}$ for all j, and it has quadratic dependence between the operating frequency deviations with respect to the target otherwise.

2) Feature-Based Objective Function for Bandwidth Maximization

The objective function for bandwidth maximization is more complex. For a single-band case, it takes the form of

$$U_F(\boldsymbol{P}(\boldsymbol{x})) = -B(\boldsymbol{x}) + \beta_b c_b(\boldsymbol{x})^2 \tag{15}$$

where the bandwidth (here, symmetric w.r.t. the center frequency $f_c = (f_L + f_R)/2$) is defined as

$$B(\boldsymbol{x}) = 2\min\{f_c - f_{B.L}, f_{B.R} - f_c\} \tag{16}$$

The bandwidth-defining frequencies $f_{B.L}$ and $f_{B.R}$ are

$$f_{B.L} = \begin{cases} f_{L/2} & \text{if } l_{\min} > -10 \text{ dB} \text{ or } \dfrac{f_{-10.L} - f_{L/2}}{f_{R/2} - f_{L/2}} > \dfrac{1}{3} \\ f_{-10.L} & \text{otherwise} \end{cases} \tag{17}$$

$$f_{B.R} = \begin{cases} f_{R/2} & \text{if } l_{\min} > -10 \text{ dB} \text{ or } \dfrac{f_{R/2} - f_{-10.R}}{f_{R/2} - f_{L/2}} > \dfrac{1}{3} \\ f_{-10.R} & \text{otherwise} \end{cases} \tag{18}$$

The reflection levels at $f_{B.L}$ and $f_{B.R}$ are $l_{B.L}$ and $l_{B.R}$, respectively (and equal to either –10 dB or to $L_{L/2}/L_{R/2}$ depending on the case in (17) and (18)). The penalty factor $c_b(\boldsymbol{x})$ in (15) is to ensure that the antenna reflection does not exceed –10 dB within its operating bandwidth. We have

$$c_b(\boldsymbol{x}) = \max\left\{\max\{l_{B.L}(\boldsymbol{x}), l_{B.R}(\boldsymbol{x}), l_{\max.1}(\boldsymbol{x}), \ldots\} + 10, 0\right\} \tag{19}$$

The reason for the particular definition of the bandwidth-defining frequencies in (17) and (18) is that—in some cases—the –10-dB points $\boldsymbol{p}_{-10.L}$ and $\boldsymbol{p}_{-10.R}$ do not give a proper account for the bandwidth, either because these point may not exist (if $l_{\min} > -10$), or because of a specific shape of the reflection characteristic (cf. Fig. 6). Eventually, i.e., when close to the optimum, the bandwidth will be determined by $\boldsymbol{p}_{-10.L}$ and $\boldsymbol{p}_{-10.R}$.

A practical problem related to (17) and (18) is that $f_{B.L}$ and $f_{B.R}$ are discontinuous with respect to $\boldsymbol{x}$ whenever there is a jump from –10 dB frequencies to $f_{L/2}$ or $f_{R/2}$. This would be troublesome from the point of view of numerical optimization. The following formulas provide the alternative versions which are smooth with respect to $\boldsymbol{x}$, therefore more suitable for handling by numerical procedures, especially gradient-based algorithms:

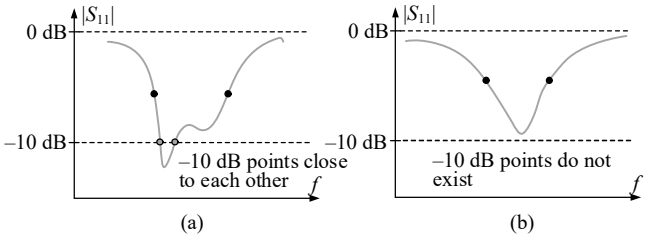

Fig. 6. Exemplary situations when a better account for the impedance bandwidth can be obtained using the frequencies $f_{L/2}$ and $f_{R/2}$ rather than –10-dB points: (a) the –10-dB points are very close to each other, (b) the –10-dB points do not exist. Both cases motivate the definitions (17) and (18) of the frequencies $f_{B.L}$ and $f_{B.R}$.

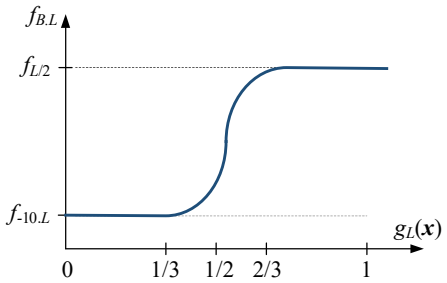

Fig. 7. Functional dependence of $f_{B.L}$ on $g_L(\boldsymbol{x})$ according to (20).

$$f_{B.L} = \begin{cases} f_{-10.L} & \text{if } g_L(\boldsymbol{x}) \le 1/3 \\ f_{-10.L} + 0.5\left(f_{L/2} - f_{-10.L}\right)\left[6(g_L(\boldsymbol{x}) - 1/3)\right]^2 & \\ \text{if } 1/3 < g_L(\boldsymbol{x}) \le 1/2 & \\ f_{L/2} - 0.5\left(f_{L/2} - f_{-10.L}\right)[6(2/3 - g_L(\boldsymbol{x}))]^2 & \\ \text{if } 1/2 < g_L(\boldsymbol{x}) \le 2/3 & \\ f_{L/2} \text{ if } 2/3 < g_L(\boldsymbol{x}) & \end{cases} \tag{20}$$

where $g_L(\boldsymbol{x}) = [f_{-10.L} - f_{L/2}]/[f_{R/2} - f_{L/2}]$ (here, $f_{-10.L} = f_{\min}$ if $l_{\min} > -10$ dB), and

$$f_{B.R} = \begin{cases} f_{-10.R} & \text{if } g_R(\boldsymbol{x}) \le 1/3 \\ f_{-10.R} + 0.5\left(f_{R/2} - f_{-10.R}\right)\left[6(g_R(\boldsymbol{x}) - 1/3)\right]^2 & \\ \text{if } 1/3 < g_R(\boldsymbol{x}) \le 1/2 & \\ f_{R/2} - 0.5\left(f_{R/2} - f_{-10.R}\right)[6(2/3 - g_R(\boldsymbol{x}))]^2 & \\ \text{if } 1/2 < g_R(\boldsymbol{x}) \le 2/3 & \\ f_{R/2} \text{ if } 2/3 < g_R(\boldsymbol{x}) & \end{cases} \tag{21}$$

where $g_R(\boldsymbol{x}) = [f_{R/2} - f_{-10.R}]/[f_{R/2} - f_{L/2}]$ (here, $f_{-10.R} = f_{\min}$ if $l_{\min} > -10$ dB). Figure 7 shows the functional dependence of $f_{B.L}$ on $g_L(\boldsymbol{x})$.

Generalization of (15)-(21) for the case of multi-band antennas is straightforward. The details are omitted for the sake of brevity.

E. Generalized Response Features: Algorithm Flow

This section briefly summarizes the operation of the optimization procedure involving generalized response features. The algorithm flow has been shown in Fig. 8. Design specifications are used to define the feature points (cf. Section II.*C*), and the feature-based objective function (cf. Section II.*D*).

This article has been accepted for publication in a future issue of this journal, but has not been fully edited. Content may change prior to final publication. Citation information: DOI 10.1109/TAP.2021.3137405, IEEE Transactions on Antennas and Propagation

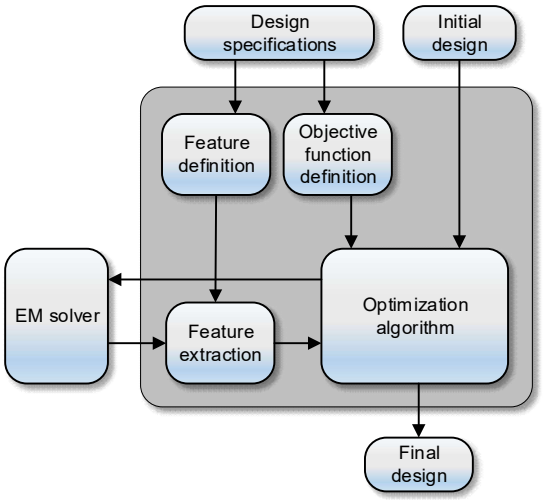

Fig. 8. Optimization using generalized response features: algorithm flow. The response feature part is pertinent to the design task formulation and EM simulation results post-processing as discussed in Sections II.*C* and II.*D*. The optimization algorithm is an independent part of the process. In this work, a trust-region gradient-based procedure is employed for all verification cases of Section III.

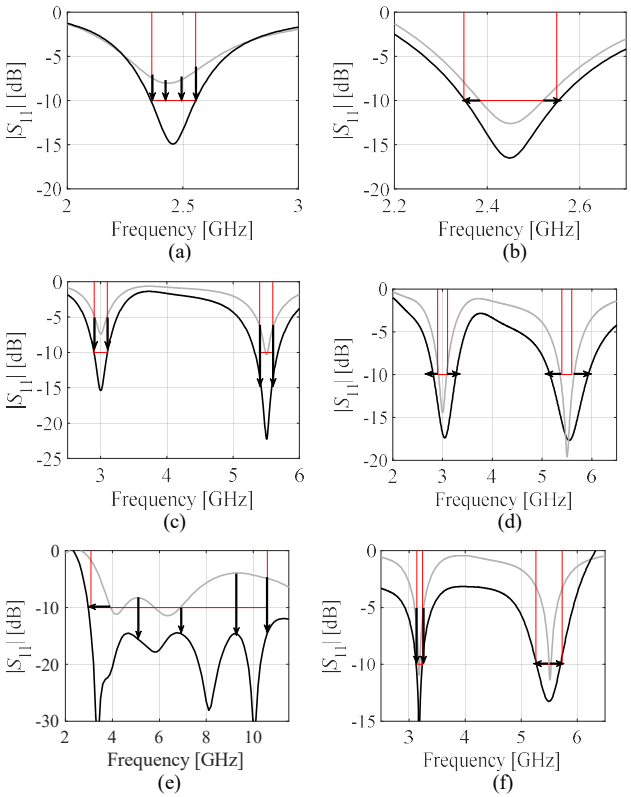

Fig. 9. A variety of the optimization tasks that may be handled in a unified manner regardless of the particular type of antenna characteristics within the proposed optimization approach using the generalized formulation of response features: (a) a single-band antenna optimized for improved matching, (b) a single-band antenna optimized for bandwidth enhancement, (c) a dual-band antenna optimized for improved matching in both operating bands, (d) a dual-band antenna optimized for bandwidth enhancement in both bands, (e) a wide-band antenna optimized for improved matching within the target operating bandwidth, (f) a dual-band antenna optimized for improved matching at and around the first operating frequency and, at the same time, optimized for bandwidth enhancement at and around the second operating frequency; the initial and optimal designs are marked gray and black, respectively, horizontal and vertical lines indicate the design specifications.

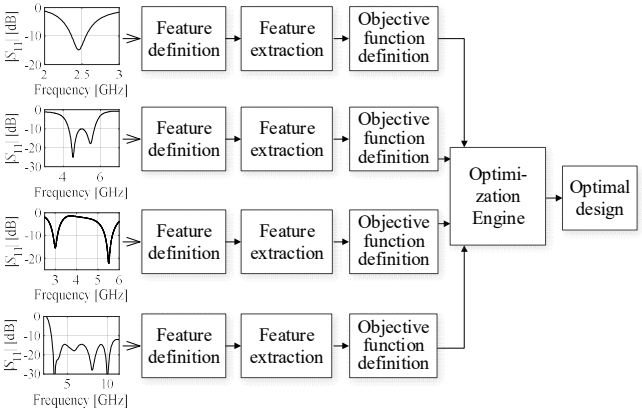

Fig. 10. Conceptual illustration of the optimization process flow according to the conventional response features approach; from left to right: (i) optimized antenna input characteristics of various types, (ii) definition of individual response features, (iii) feature extraction procedure ((ii) and (iii) are mandatory in the conventional response feature approach or for bandwidth enhancement within the conventional approach), (iv) definition of the objective function that encodes design specifications (has to be carried out separately for each design task and each antenna type), (v) design optimization routine of choice, (vi) the optimal solution.

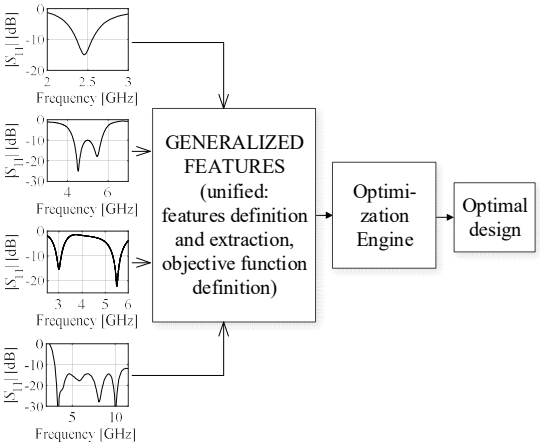

Fig. 11. Conceptual illustration of the optimization process flow in the generalized response features approach proposed in this work; from left to right: (i) optimized characteristics of various types, (ii) generalized features procedure that handles: response features definition and extraction, as well as unified objective function definition, (iii) design optimization routine of choice, (iv) the optimal solution.

The feature points are extracted from EM simulation responses each time a specific design is to be evaluated by the optimization algorithm. Using this data, the objective function value is computed. The optimization algorithm itself is an independent part of the procedure. In the numerical experiments discussed in Section III, the trust-region (TR) gradient-search [56] is employed.

It should be noted that although the unified definition of the feature points (Section II.*C*) as well as the defining details of the feature-based objective functions (Section II.*D*) may seem complex, both the feature extraction and objective function technicalities, once implemented, are hidden from the user.

As mentioned before, such a generalization is the main purpose of this work so that the same routines can be used regardless of the particular type of antenna characteristics (narrow-band, broadband, multi-band) to both extract the

This article has been accepted for publication in a future issue of this journal, but has not been fully edited. Content may change prior to final publication. Citation information: DOI 10.1109/TAP.2021.3137405, IEEE Transactions on Antennas and Propagation

feature points and to translate the performance specifications into mathematically rigorous cost functions that adequately assess the design quality and can be directly employed by the optimization algorithms.

III. Demonstration Case Studies

This section provides a numerical verification of the unified feature based optimization (FBO) technique in the context of design optimization of antenna input characteristics of various types. The numerical studies are carried out using four planar structures of distinct reflection responses: a ring slot antenna, a patch antenna with enhanced bandwidth, a multi-band dipole antenna, and an ultra-wideband monopole.

All the verification structures have been optimized for best in-band matching, whereas the ring-slot antenna has been also optimized for bandwidth enhancement. The same routines implementing the feature point extraction and objective functions are employed in each case showing the versatility of the presented approach. The feature-based formulation is compared to the conventional ways of representing the performance specifications (mostly minimax), so that the benefits of generalized FBO in terms of design reliability but also computational efficiency can be identified.

Our approach is benchmarked against the following methods: (i) gradient-based TR algorithm [56], (ii) derivative-free pattern search algorithm [57] (the specific implementation used here, described in [58], is a stencil-based procedure with variable grid size enhanced by grid-constrained line search), as well as (iii) particle swarm optimizer (PSO) [59]. The first two algorithms are local search procedures, whereas the third is a global nature-inspired population-based routine.

Figure 9 presents a selection of a variety of optimization tasks of the antenna input characteristics that the proposed approach is capable of handling without introducing any adjustments pertaining to the objective function formulation otherwise unavoidable in the conventional approach. These include:

- Optimization for the best in-band matching in the assumed target operating band of a single-band antenna (Fig. 9(a)),
- Optimization of the aforementioned structure for bandwidth enhancement (Fig. 9(b)),
- Minimization of a dual-band antenna reflection coefficient in both operating bands (Fig. 9(c)),
- Maximization of the bandwidths of the same antenna (Fig. 9(d)),
- Optimization for improved matching of a wide-band antenna within the target operation bandwidth (Fig. 9(e)),
- Optimization of a dual-band antenna for improved matching at and around the first operating frequency and, at the same time, for bandwidth enhancement at and around the second operating frequency (Fig. 9(f)).

In order to demonstrate the benefits offered by the proposed framework using a unified definition of the response features, a comparison of the optimization flow arrangement is discussed for the conventional FBO approach involving individualized response features definition of [47] (Fig. 10), and the approach proposed in this work (Fig. 11). The former requires that the designer separately handles any specific type of antenna structure and its corresponding response, which entails individual definition and extraction of the feature points (including implementation of the relevant Matlab codes, etc.), cf. Fig. 10. Subsequently, the designer needs to define the objective function encoding the design specifications. Whereas in the proposed approach, as shown in Fig. 11, the generalized features procedure handles all the response types and the design tasks in a unified and automated manner. Thus, the response features definition and extraction, as well as the definition of the merit function is carried out without the designer's interaction, which streamlines the entire design process.

The aim of the paper is to propose an optimization framework for reliable and efficient antenna design, therefore, the experimental validation of the benchmark verification structures is considered irrelevant. Interested reader can find measurement data in prior works (e.g., [60]-[63]).

A. Example I: Ring Slot Antenna

Our first example is a slot antenna shown in Fig. 12 [64]. The structure is implemented on a 0.76-mm-thick substrate of relative permittivity $\varepsilon_r = 3.5$. The antenna is excited through a microstrip line, which feeds a circular ground plane slot with defected ground structure [64]. The designable variables are $\boldsymbol{x} = [l_f\ l_d\ w_d\ r\ s\ s_d\ o\ g]^T$. The unit for all the parameters is millimeter. The feed line width w_f is adjusted to achieve 50 ohm input impedance. The lower and upper bounds for the design variables are: $\boldsymbol{l} = [20\ 1\ 0.2\ 6.5\ 0.2\ 0.2\ 1\ 0.2]^T$ and $\boldsymbol{u} = [35\ 10\ 2.2\ 15.5\ 7.0\ 7.0\ 12\ 4]^T$, respectively. The EM simulation model is evaluated in CST (~300,000 cells, simulation 90 s). The antenna has been optimized for: (i) the best in-band matching around the center frequency f_0, and (ii) enhanced impedance bandwidth around f_0.

The first design task is to improve antenna matching at the target operating frequency f_0. The numerical experiments have been performed for the following two values of the operating frequency: $f_0 = 2.45$ GHz and $f_0 = 5.3$ GHz. Figure 13 shows the designs optimized within the proposed approach, as well those rendered using the conventional local search procedures: trust region and pattern search algorithm, starting from four different initial designs. The optimal designs shown in Figs. 13(a) and 13(c) satisfy the assumed specifications for both the approaches. Whereas the conventional TR local search starting from the initial designs distant from the required target operating frequencies fails to find satisfactory designs (see Figs. 13(b) and 13(d)). As for the pattern search algorithm, it has been capable of appropriately allocating the operating frequency in three out of four cases, and failed only in the case of the design of Fig. 13(b). Notwithstanding, the procedure of Section II is capable of accurately allocating target operating frequencies in all considered cases. As the objective function is defined differently in both approaches, for comparison purposes, we quantify the design quality as the maximum reflection level at f_0. For the designs yielded in our approach (shown in Fig. 13) the average value is –17.1 dB, whereas for the TR algorithm it is –14.0 dB, and –12.5 dB in the case of pattern search algorithm.

This article has been accepted for publication in a future issue of this journal, but has not been fully edited. Content may change prior to final publication. Citation information: DOI 10.1109/TAP.2021.3137405, IEEE Transactions on Antennas and Propagation

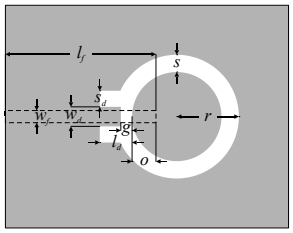

Fig. 12. Geometry of a ring-slot antenna; dashed lines mark feeding line [64].

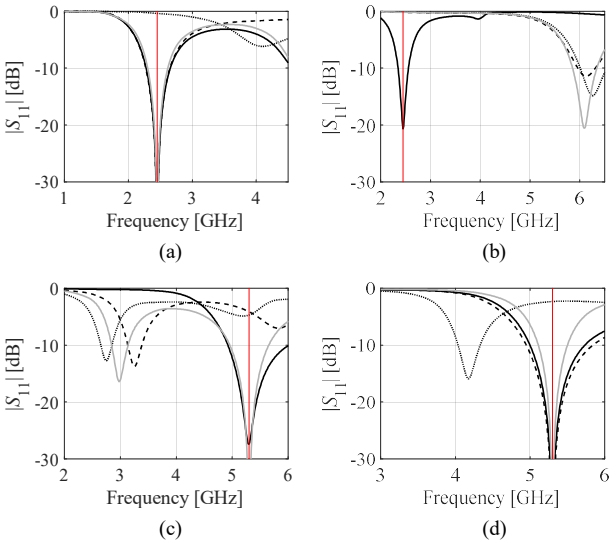

Fig. 13. Ring-slot antenna of Fig. 12, optimization for best in-band matching. Shown are the responses: at the initial design (····), the design optimized using the proposed algorithm exploiting generalized formulation of response features (—), the design optimized using classic TR algorithm (- - -), and the design optimized using the conventional pattern search algorithm (gray). The presented designs correspond to the following target operating frequencies: (a), (b) f_0 = 2.45 GHz, (c), (d) f_0 = 5.3 GHz and have been optimized staring from different initial designs. Vertical lines indicate the design specifications.

The respective computational costs equal 152, 72, and 338 EM analyses (i.e., the cost of design optimization using the pattern search algorithm is the highest among the compared local procedures, over twice as much as the proposed technique). Yet, perhaps the most important factor that allows for comparing both the approaches is the accuracy of the operating frequency allocation. In our approach, the average error of the operating frequency misalignment (for the designs of Fig. 13) equals merely 2.6 percent, whereas in the conventional approaches, it is as high as 91.9 and 91.0 percent, for TR and pattern search algorithm, respectively. This corroborates suitability of the proposed generalized features optimization framework for reliable antenna design.

Figure 14 shows the results of maximizing the bandwidth for the ring-slot antenna of Fig. 12 using our methodology. As before, the optimal designs meet the assumed design specifications. It should be observed that—within the conventional local approach (both TR and pattern search algorithms)—the bandwidth enhancement cannot be performed without some kind of feature definition (as well as extraction) for assessing the antenna bandwidth at each iteration of the optimization algorithm run.

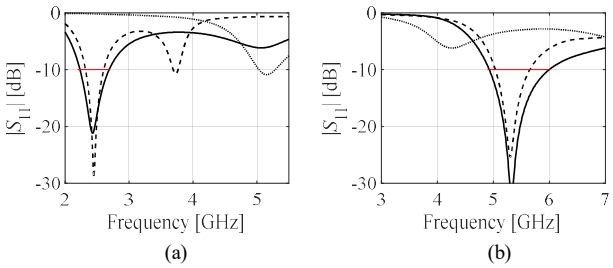

Fig. 14. Ring-slot antenna of Fig. 12, optimization for bandwidth enhancement (observe that this kind of optimization task cannot be directly carried out within the classical approach). Responses of ring-slot antenna at the designs optimized using the proposed algorithm exploiting generalized formulation of response features: the initial design (····), the design optimized for enhanced bandwidth (—), and the design optimized for the best in-band matching (- - -). Shown are the designs corresponding the target operating frequency f_0 = 2.45 GHz and f_0 = 5.3 GHz. Horizontal lines mark the design specifications.

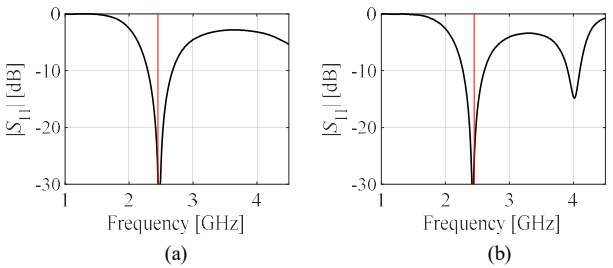

Fig. 15. Ring-slot antenna of Fig. 12, optimization for the best in-band matching at f_0 = 2.45 GHz using PSO benchmark algorithm (—). Shown are representative optimal designs. Vertical lines indicate design specifications.

For comparison purposes, Fig. 15 provides the selected optimal designs for best in-band matching at f_0 = 2.45 GHz rendered by multiple runs (ten) of the benchmark particle swarm optimization (PSO) procedure (population size of 20, maximum number of iterations equal to 50). The quality of the PSO-optimized designs is very good (the maximum reflection at f_0 is –27.7 dB on average, with the standard deviation of 2.2 dB across ten algorithm runs). The accuracy of the operating frequency is excellent and equals 1.0 percent. Yet, this is achieved at the computational cost that equals 1000 EM analyses which is significantly higher (by a factor of about ten) than that of the local search (both classical and the proposed one).

B. Example II: Triple-Band Dipole Antenna

Our second verification case is a triple-band dipole antenna shown in Fig. 16 [61]. The structure is fed by a coplanar waveguide, and implemented on RO4350 substrate (ε_r = 3.48, h = 0.762 mm). The geometry parameters are: $\boldsymbol{x} = [l_1\ l_2\ l_3\ l_4\ l_5\ w_1\ w_2\ w_3\ w_4\ w_5]^T$. The following dimensions l_0 = 30, w_0 = 3, s_0 = 0.15 and o = 5 remain fixed. All dimensions are expressed in mm. The lower and upper bounds on the design variables are: $\boldsymbol{l}$ = [30 5 20 5 15 0.2 0.2 0.2 0.2 0.2]^T and $\boldsymbol{u}$ = [50 15 30 14.9 21 2.2 4.2 2.2 4.2 2.2] ^{T}, respectively. The computational model is simulated in CST Microwave Studio using its time-domain solver. The antenna is intended to operate within 50 MHz bandwidths around the following center frequencies: 2.45 GHz, 3.6 GHZ and 5.3 GHz.

This article has been accepted for publication in a future issue of this journal, but has not been fully edited. Content may change prior to final publication. Citation information: DOI 10.1109/TAP.2021.3137405, IEEE Transactions on Antennas and Propagation

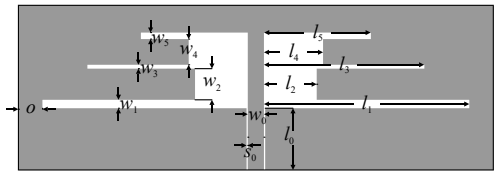

Fig. 16. Geometry of the triple-band dipole antenna [61].

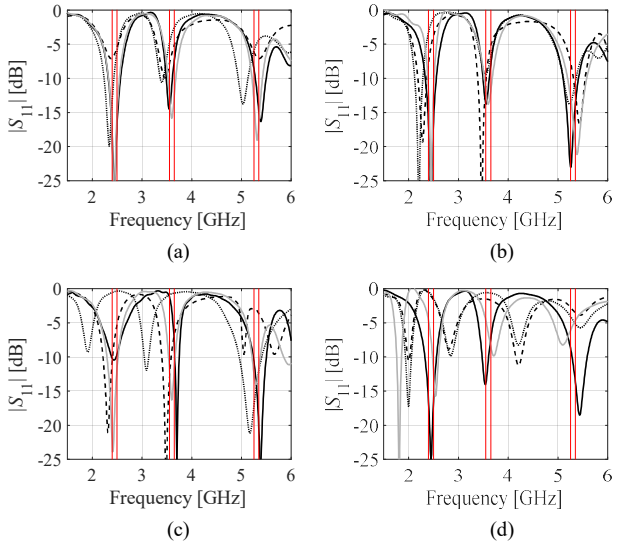

Fig. 17. Triple-band antenna of Fig. 14, optimization for the best in-band matching at the ±50 MHz bands centered at 2.45 GHz, 3.6 GHz and 5.3 GHz. Shown are the responses: at four different initial designs (a) through (d) (····), the designs optimized using the proposed algorithm exploiting generalized formulation of response features (—), the designs optimized using classic TR algorithm (- - -), and the designs optimized using the conventional pattern search algorithm (gray). Vertical lines indicate design specifications.

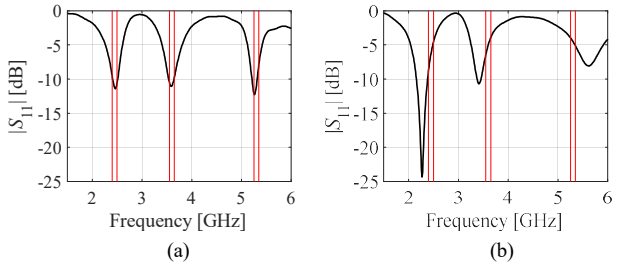

Fig. 18. Triple-band antenna of Fig. 14, optimization for the best in-band matching at the ±50 MHz bands centered at 2.45 GHz, 3.6 GHz and 5.3 GHz using PSO benchmark algorithm (—). Shown are two selected PSO-optimized designs featuring: (a) correctly allocated operating frequencies, (b) operating frequencies misaligned with respect to the assumed design specifications (marked with vertical lines).

Figure 17 shows the designs optimized within the classical and the proposed approach for the triple-band antenna of Fig. 16. The results of Fig. 17 show superiority of our algorithm over the benchmark: the target operating frequencies of all the optimized designs are allocated accurately. Whereas the optimal designs rendered by classical local search TR procedure are considerable misaligned with the target in all presented cases. As far as pattern search algorithm is concerned, it has been capable of allocating the operating frequencies in three out of four cases. The respective errors of the target frequency allocation equal 1.6 percent (our approach), 26.2 percent (TR approach), and 27.4 percent (pattern search algorithm). The design quality (quantified as the maximum reflection level at the center frequencies) is –11.8 dB, –3.9 dB, and –12.0 dB (the proposed, TR and pattern search approaches, respectively) on the average, across the design set of Fig. 17. The corresponding CPU cost is 76.3, 85.7 and 730 EM analyses, respectively. As before, the cost of pattern search algorithm is the highest (around ten times higher than that of the proposed procedure) among local routines.

For additional verification, Fig. 18 presents the designs optimized with the use of PSO (selected from the ten algorithm runs). The operating frequencies of the antenna of PSO-rendered designs are allocated accurately for the design of Fig. 18(a), yet, they are considerably misaligned for the design shown in Fig. 18(b). The average maximum reflection around at the operating frequencies is –7.0 dB, with the standard deviation of 2.5 dB. The average accuracy of the operating frequencies allocation is slightly worse than in our approach and equals to 1.8 percent. Still, one has to bear in mind the tremendous cost of optimizing these designs (1000 EM simulations), considerably (over ten times) higher than that of the proposed technique.

C. Example III: Bandwidth-Enhanced Patch Antenna

Our third example is a bandwidth-enhanced planar antenna presented in Fig. 19 [62]. The structure comprises two radiating elements in the form of a quasi-microstrip patch with inset feed excited through a microstrip line. The antenna is implemented on 0.76-mm-thick substrate of relative permittivity $\varepsilon_r = 3.0$, $\tan\delta = 0.0018$. The independent geometry parameters are $\boldsymbol{x} = [L\ l_1\ l_2\ l_3\ W\ w_1\ w_2\ g]^T$. Whereas the following parameters are fixed: $o = 7$, $l_0 = 10$ *and* $s = 0.5$. *The lower and upper bounds on design* variables are: $\boldsymbol{l} = [10\ 0.1\ 5\ 0.1\ 2\ 0.2\ 0.1\ –6]^T$, and $\boldsymbol{u} = [40\ 10.0\ 30\ 15\ 30\ 8\ 15\ 15]^T$, respectively. The unit for all dimensions is mm. The feed line width w_0 is adjusted to ensure 50-ohm impedance. The EM antenna model is implemented in CST Microwave Studio.

The antenna has been optimized for the best in-band matching within the frequency range 4.5 GHz ≤ f ≤ 5.5 GHz. Figure 20 shows the designs optimized using our methodology, along with those optimized using classical TR gradient-based search and pattern search procedure. In three out of four cases, the proposed approach outperforms both benchmark local procedures in terms of allocating the target bandwidth. It should be emphasized that the initial designs are considerably misaligned with respect to the target bandwidth, yet, the proposed technique has been capable of finding the optimal solutions satisfying the design specifications. The average value of the maximum of the input reflection characteristic within the target bandwidth is –15.8 dB for the proposed approach, as well as –9.9 dB and –1.1 dB for the local benchmark procedures, respectively (across the set of designs of Fig. 20). The computational cost of rendering the optimal designs is comparable for our and TR approach and it equals to 113.8 and 110.5 EM simulations per design, respectively. Whereas in the case of pattern search algorithm it is significantly higher and equals to 585 EM analyses (i.e., it is over five times higher).

This article has been accepted for publication in a future issue of this journal, but has not been fully edited. Content may change prior to final publication. Citation information: DOI 10.1109/TAP.2021.3137405, IEEE Transactions on Antennas and Propagation

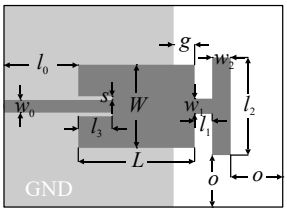

Fig. 19. Geometry of the planar antenna with enhanced bandwidth [62]. Ground plane marked using light gray shade.

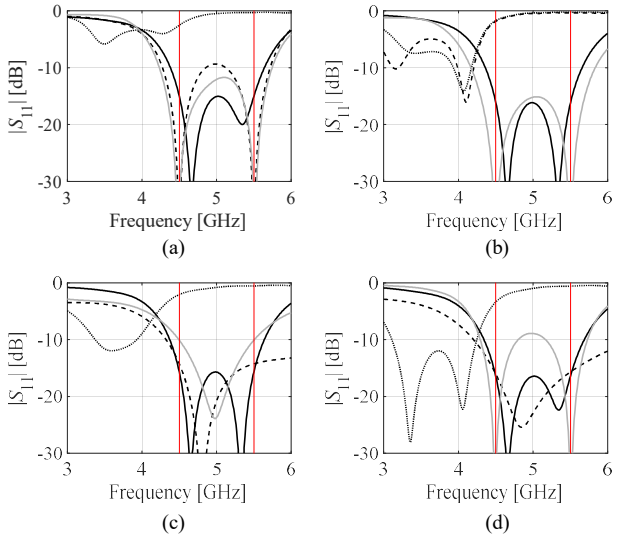

Fig. 20. Bandwidth-enhanced patch antenna of Fig. 19, optimization for the best in-band matching within the frequency range 4.5 GHz ≤ f ≤ 5.5 GHz. Shown are the responses: at four different initial designs considerably misaligned with the target bandwidth (····), the designs optimized using the proposed algorithm exploiting generalized formulation of response features (—), the design optimized using classic TR algorithm (- - -), and the design optimized using the conventional pattern search algorithm (gray). Vertical lines indicate design specifications.

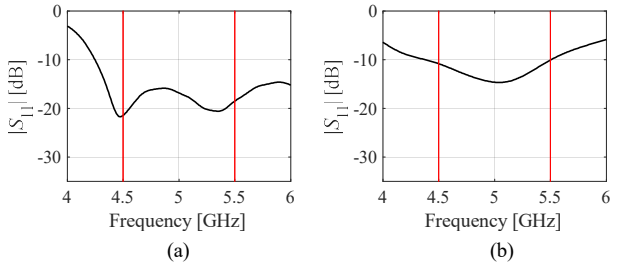

Fig. 21. Bandwidth-enhanced patch antenna of Fig. 19, optimization for the best in-band matching within the frequency range 4.5 GHz ≤ f ≤ 5.5 GHz using PSO benchmark algorithm (—). Shown are representative optimized designs. Vertical lines indicate design specifications.

Similarly as for the previous examples, Fig. 21 provides the exemplary optimal designs rendered with PSO optimization algorithm. One of them accurately allocates the antenna operating bandwidth (from 4.5 GHz to 5.5 GHz), whereas the other is considerably misaligned. The average quality of PSO-rendered designs equals –12.9 dB, with the standard deviation of 4.1 dB (across ten algorithm runs). The operational bandwidth has been properly allocated at six out of ten optimal designs. Nevertheless, the cost of rendering these designs is equal to 1000 EM analyses, which is—again—around ten times higher than that of the local search.

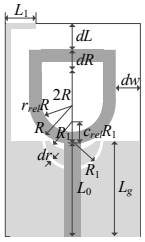

Fig. 22. Geometry of the ultra-wideband antenna [65]. Ground plane marked using light gray shade.

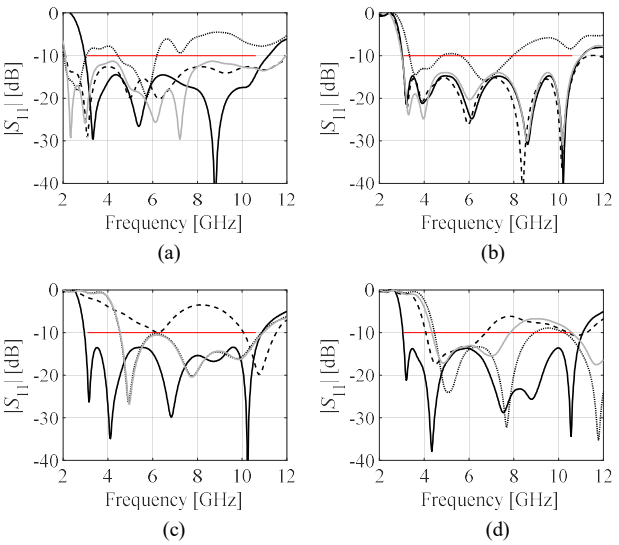

Fig. 23. Broadband antenna of Fig. 21, optimization for best in-band matching within UWB band from 3.1 GHz to 10.6 GHz. Shown are the responses: at the initial designs (····), the designs optimized using the proposed algorithm exploiting generalized formulation of response features (—), the designs optimized using classic TR algorithm (- - -), and the designs optimized using the conventional pattern search algorithm (gray). Vertical line indicates the design specifications.

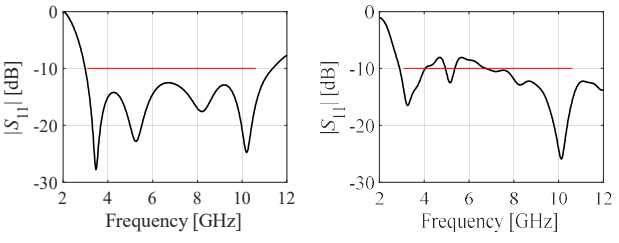

Fig. 24. Broadband antenna of Fig. 21, optimization for best in-band matching within UWB band from 3.1 GHz to 10.6 GHz using PSO benchmark algorithm (—). Shown are two designs: (a) meeting the assumed design specifications (marked with horizontal line), and (b) with $|S_{11}|$ exceeding the level of –10dB in a part of the UWB frequency range.

D. Example IV: Ultra-wideband Antenna

The last verification case is an ultra-wideband antenna implemented on Taconic RF-35 substrate (h = 0.762 mm, ε_r = 3.5, tanδ = 0.0018) shown in Fig. 22 [65]. The structure employs a quasi-circular radiator, along with a modified ground plane for bandwidth enhancement. The antenna geometry parameter vector is $\boldsymbol{x} = [L_0\ dR\ R\ r_{rel}\ dL\ dw\ L_g\ L_1\ R_1\ dr\ c_{rel}]^T$. The lower and upper bounds on the parameters are: $\boldsymbol{l} = [4.0\ 0\ 3.0\ 0.1\ 0\ 0\ 4.0\ 0\ 2.0\ 0.2\ 0.2]^T$, and $\boldsymbol{u} = [15.0\ 6.0\ 8.0\ 0.9\ 5.0\ 8.0\ 15.0\ 6.0$

This article has been accepted for publication in a future issue of this journal, but has not been fully edited. Content may change prior to final publication. Citation information: DOI 10.1109/TAP.2021.3137405, IEEE Transactions on Antennas and Propagation

5.0 1.0 0.9]^T, all dimensions in mm. The antenna is to be optimized for minimum reflection within the UWB frequency range (3.1 GHz to 10.6 GHz).

Figure 23 shows the optimal designs for antenna of Fig. 22. rendered in the proposed approach, as well as those obtained using the benchmark local TR and pattern search algorithms. The results indicate that our method allows for meeting the design specifications in all the considered cases, whereas the TR algorithm is not capable of assigning the antenna bandwidth accurately, especially when the initial design is allocated over the intended frequency range (see Figs. 23(c) and 23(d)), the same pertains to the pattern search procedure. The average computational cost of rendering the designs of Fig. 22 is 125.5, 83.5 and 598 EM simulations for our, TR and pattern search algorithms, respectively. The corresponding design quality (maximum value of the reflection characteristic within the UWB range) is –14.7 dB, –7.51 dB and –6.7 dB, respectively. Again, the cost of the pattern search procedure is the highest one (around five times higher than that of the feature-based technique).

As a supplementary verification, the broadband antenna of Fig. 22 has also been optimized with the PSO algorithm (see Fig. 24). One of the presented PSO-optimal designs is of high-quality: the intended UWB bandwidth is allocated accurately and the reflection does not exceed –10 dB level (Fig. 23(a)). However, this is not the case for the design shown in Fig. 23(b), which exceeds the assumed reflection level. The cost of rendering both the designs shown in Fig. 24 is as high as 1000 EM analyses. The average design quality (maximum in-band reflection) is –10.9 dB (i.e., it is poorer than within our approach), with standard deviation of 1.8 dB across 10 algorithm runs. The maximum reflection level of the PSO-rendered designs does not exceed –10 dB level for 7 out of 10 designs.

E. Discussion

The analysis of the results presented in Section III.*A* through III.*D* allows us to draw several conclusions concerning the advantages offered by the proposed optimization algorithm exploiting the unified and automated definition of response features, as well as the performance of the proposed procedure when compared to that of the conventional local search and particle swarm optimization algorithm. The observations can be summarized as follows:

- The proposed approach has been demonstrated to successfully handle a variety of antenna structures featuring different types of input characteristics while using identical setup with no need of user interaction;
- The allocation and extraction of the feature points is automated with the only information provided by the user being design specifications;
- Based on the same information, the procedure selects and sets up the appropriate feature-based objective function, again, without engaging the expert knowledge of the user;
- The results confirm the reliability of our approach: for all of the verification structures, the optimal designs satisfy the assumed specifications, even for severely misaligned initial designs;
- The conventional local trust-region gradient search algorithm frequently fails to find the optimal designs meeting the target operating frequencies and it is very much dependent on the quality of the start point;
- The pattern search algorithm (the second local benchmark procedure), also is incapable of yielding the designs that satisfy the specifications in some of the presented cases, and its outcome heavily depends on the antenna operating frequencies at the intial design. In addtion, it incurs the highest computational cost among the three local optimizers (from five to even ten times higher, depending on the structure);
- The considered problems are generally challenging even for state-of-the-art nature-inspired procedures (here, represented by PSO). The PSO-rendered optimal designs for some structures do not meet the assumed design specifications, which puts its reliability in question;
- The quality of the optimal designs rendered by all the compared procedures (the proposed one, conventional local algorithms: TR and pattern search, as well as PSO optimizer) is similar across the set of four benchmark antenna structures of different types of input characteristics (provided the local and PSO optimizer have been able to identify these);
- The computational cost of the proposed procedure is—on the average—comparable (or slightly higher) that that of the conventional TR approach, and considerably lower than that of the pattern search algorithm. Still, even though the TR local search is in some cases faster, its reliability is significantly inferior to that of our approach;
- The computational cost of our procedure is around ten times smaller than for the PSO algorithm while providing optimal designs of similar quality.

The overall conclusion is that the performance of the optimization process is greatly improved by employing the generalized definition of the response features. The execution of the entire procedure is facilitated by the unified feature definition and extraction, but also unified objective function formulation. Comprehensive validation studies demonstrate that generalized response feature technology allows for obtaining high quality designs, even when starting from poor initial parameter vectors, normally call requiring the employment of global procedures. Moreover, the proposed procedure is computationally efficient with the cost comparable to conventional local TR procedure, a fraction (ten to twenty percent) of the cost of pattern search algorithm, and about ten percent of that of the particle swarm optimizer. The most important observation is that the generalization introduced in this work performs up to the expectations and the purpose it was developed for, especially in terms of handling a variety of design tasks and types of antenna input characteristics within a single and automated algorithmic framework.

This article has been accepted for publication in a future issue of this journal, but has not been fully edited. Content may change prior to final publication. Citation information: DOI 10.1109/TAP.2021.3137405, IEEE Transactions on Antennas and Propagation

IV. Conclusion

This paper proposed a generalized formulation of the response feature technology for efficient and reliable optimization of antenna input characteristics of various types. The presented approach unifies different definitions used so far in the literature to determine the characteristic points of antenna responses and provides a single framework, suitable for handling narrow-, multi-band, enhanced bandwidth, as well as broadband (also ultra-wideband) structures. The generalized definition of response features is accompanied by a unified formulation of the feature-based objective functions that cover the design tasks related to in-band matching improvement and bandwidth enhancement. The major advantage of our methodology is that it eliminates the need for defining both the response features and the cost functions individually for a particular antenna structure. Thus, it makes the feature-based optimization (FBO) more accessible for an inexperienced user.

A comprehensive numerical verification demonstrates the performance of the method over a range of antenna structures featuring different types of input characteristics (ring-slot, triple-band dipole, enhanced-bandwidth patch antenna, and ultra-wideband monopole antenna) but also corroborates other advantages of FBO, which include the improved reliability (in particular, good performance when facing poor initial design) and reduced computational cost as compared to the standard design problem definitions. The presented formulation has been specifically developed for handling antenna input characteristics. Generalizations for antenna responses such as gain, axial ratio, etc. (i.e., other than input characteristics), as well as for compound problems (e.g., gain maximization under reflection constraints, or simultaneous impedance matching and axial ratio bandwidth improvement) will be addressed in the future work.

All the aforementioned benefits are achieved at the expense of limiting the scope of applicability of the modelling method to structures whose responses feature well distinguished characteristic points, e.g., the aforementioned multi-band antennas. As a result, the proposed methodology is not as versatile as other frameworks that do not impose any restraints on the response structure of the component under design. Yet, the characteristics of many real-world antennas are inherently structured (e.g., narrow-band or multi-band antennas). Consequently, the employment of the feature-based techniques is not hindered by the aforementioned factors.

Having said that, by unifying the definition of response features, the proposed technique overcomes some of the limitations of the prior versions, all of which exploited individual (i.e. problem-specific) definitions of the characteristic points. The application of the latter has been significantly limited to such antenna structures whose responses featured readily discernible characteristic points (e.g., multi-band antennas). Therefore, such frameworks have been not as versatile as other procedures capable of handling antenna responses of arbitrary shapes.

The technique discussed in this work can be considered a step towards extending the applicability of the response feature technology for antenna design. It can be of interest, among others, for the readers dealing with simulation-driven optimization tasks that are difficult to handle by means of conventional local optimization algorithms, yet, for which the use of global search routines may be impractical from the point of view of their computational complexity. It is also useful whenever the antennas need to be re-designed with respect to their operating frequencies because FBO is a practical tool for manipulating the antenna resonances/bandwidth in a convenient manner. Finally, it should be mentioned that the feature-based optimization concept can also be generalized for handling other types of high-frequency structures, including microwave components. Notwithstanding, such a generalization is a more challenging endeavor due to a larger variety of possible system outputs (e.g., pertinent to filters, couplers, power dividers, etc.) that need to be taken into account by a respective framework.

Acknowledgment

The authors would like to thank Dassault Systemes, France, for making CST Microwave Studio available.

References

[1] M. Rokunuzzaman, M. Samsuzzaman, and M.T. Islam, "Unidirectional wideband 3-D antenna for human head-imaging application," *IEEE Ant. Wireless Prop. Lett.*, vol. 16, pp. 169-172, 2017.

[2] Y. Liu, Z. Ai, G. Liu, and Y. Jia, "An integrated shark-fin antenna for MIMO-LTE, FM, and GPS applications," *IEEE Ant. Wireless Prop. Lett.*, vol. 18, no. 8, pp. 1666-1670, 2019.

[3] X. S. Yang, J. Wang, and B. Z. Wang, "Topology optimization of patch antennas with specified polarization and beam characteristics," *In 6th Asia-Pacific Conf. Ant. Propag.*, Xian, China, Oct. 2017.

[4] Z. Nie, H. Zhai, L. Liu, J. Li, D. Hu, and J. Shi, "A dual-polarized frequency-reconfigurable low-profile antenna with harmonic suppression for 5G application," *IEEE Ant. Wireless Prop. Lett.*, vol. 18, no. 6, pp. 1228-1232, 2019.

[5] Y. Wang, J. Zhang, F. Peng, and S. Wu, "A glasses frame antenna for the applications in internet of things," *IEEE Internet of Things J.*, vol. 6, no. 5, pp. 8911-8918, 2019.

[6] Z. Zhao, C. Pichot, and C. Dedeban, "Topological shape gradient and Level-Set method for optimizing planar antennas," *IEEE Conf. Antenna Measurements & Appl. (CAMA)*, Chiang Mai, Thailand, pp. 1-4, 2015.

[7] A. A. Al-Azza, A. A. Al-Jodah, and F. J. Harackiewicz, "Spider monkey optimization: a novel technique for antenna optimization," *IEEE Ant. Wireless Prop. Lett.*, vol. 15, pp. 1016-1019, 2016.

[8] M. Tang, X. Chen, M. Li, and R. W. Ziolkowski, "Particle swarm optimized, 3-D-printed, wideband, compact hemispherical antenna," *IEEE Ant. Wireless Propag. Lett.*, vol. 17, no. 11, pp. 2031-2035, 2018.

[9] L. A. Greda, A. Winterstein, D. L. Lemes, and M. V. T. Heckler, "Beamsteering and beamshaping using a linear antenna array based on particle swarm optimization," *IEEE Access*, vol. 7, pp. 141562-141573, 2019.

[10] P. Baumgartner, T. Baurnfeind, O. Biro, A. Hackl, C. Magele, W. Renhart, and R. Torchio, "Multi-objective optimization of Yagi-Uda antenna applying enhanced firefly algorithm with adaptive cost function," *IEEE Trans. Magnetics*, vol. 54, no. 3, paper no. 8000504, 2018.

[11] G. Ram, D. Mandal, R. Kar, and S. P. Ghoshal, "Cat swarm optimization as applied to time-modulated concentric circular antenna array: analysis and comparison with other stochastic optimization methods," *IEEE Trans. Antennas Propag.*, vol. 63, no. 9, pp. 4180-4183, 2015.

[12] M. Li, Y. Liu, and Y. J. Guo, "Shaped power pattern synthesis of a linear dipole array by element rotation and phase optimization using dynamic differential evolution," *IEEE Ant. Wireless Prop. Lett.*, vol. 17, no. 4, pp. 697-701, 2018.

[13] I. Syrytsin, S. Zhang, G. F. Pedersen, K. Zhao, T. Bolin, and Z. Ying, "Statistical investigation of the user effects on mobile terminal antennas

for 5G applications," *IEEE Trans. Ant. Prop.*, vol. 65, no. 12, pp. 6596-6605, 2017.

[14] J. Du and C. Roblin, "Statistical modeling of disturbed antennas based on the polynomial chaos expansion," *IEEE Ant. Wireless Prop. Lett.*, vol. 16, p. 1843-1847, 2017.

[15] D. I. L. de Villiers, I. Couckuyt, and T. Dhaene, "Multi-objective optimization of reflector antennas using kriging and probability of improvement," *Int. Symp. Ant. Prop.*, pp. 985-986, San Diego, USA, 2017.

[16] A. Lalbakhsh, M. U. Afzal, and K. P. Esselle, "Multiobjective particle swarm optimization to design a time-delay equalizer metasurface for an electromagnetic band-gap resonator antenna," *IEEE Ant. Wireless Propag. Lett.*, vol. 16, pp. 912-915, 2017.

[17] Y. Liu, Y. -C. Jiao, Y. -M. Zhang, and Y. -Y. Tan, "Synthesis of phase-only reconfigurable linear arrays using multiobjective invasive weed optimization based on decomposition," *Int. J. Ant. Propag.*, vol. 2014, art. no. 630529, 2014.

[18] H. Wang, C. Liu, H. Wu, B. Li, and X. Xie, "Optimal pattern synthesis of linear array and broadband design of whip antenna using grasshopper optimization algorithm," *Int. J. Ant. Propag.*, vol. 2020, art. no. 5904018, 2020.

[19] Z. Lukes and Z. Raida, "Multi-objective optimization of wire antennas: Genetic algorithms versus particle swarm optimization," *Radioengineering*, vol. 14, no. 4, pp. 91-97, 2005.

[20] B. Lin, S. Liu, and N. Yuan, "Analysis of frequency selective surfaces on electrically and magnetically anisotropic substrates," *IEEE Trans. Ant. Prop.*, vol. 54, no. 2, pp. 674-680, 2006.

[21] S. Kim and S. Nam, "A compact and wideband linear array antenna with low mutual coupling," *IEEE Trans. Ant. Prop.*, vol. 67, no. 8, pp. 5695-5699, 2019.

[22] J. Nocedal and S. J. Wright, *Numerical Optimization*, 2nd Ed., Springer, New York, 2000.

[23] M. M. T. Maghrabi, M. H. Bakr, S. Kumar, A. Z. Elsherbeni, and V. Demir, "FDTD-based adjoint sensitivity analysis of high-frequency nonlinear structures," *IEEE Trans. Ant. Prop.*, vol. 68, no. 6, pp. 4727-4737, 2020.

[24] J. Wang, X.S. Yang, and B. Z. Wang, "Efficient gradient-based optimisation of pixel antenna with large-scale connections," *IET Microwaves Ant. Prop.*, vol. 12, no. 3, pp. 385-389, 2018.

[25] CST Microwave Studio, ver. 2019, Dassault Systemes, France, 2019.

[26] S. Koziel and A. Pietrenko-Dabrowska, "Variable-fidelity simulation models and sparse gradient updates for cost-efficient optimization of compact antenna input characteristics," *Sensors*, vol. 19, no. 8, 2019.

[27] A. Pietrenko-Dabrowska and S. Koziel, „Computationally-efficient design optimization of antennas by accelerated gradient search with sensitivity and design change monitoring," *IET Microwaves Ant. Prop.*, vol. 14, no. 2, pp. 165-170, 2020.

[28] S. Koziel and A. Pietrenko-Dabrowska, "Expedited optimization of antenna input characteristics with adaptive Broyden updates," *Eng. Comp.*, vol. 37, no. 3, 2019.

[29] Q. Wu, H. Wang, and W. Hong, "Multistage collaborative machine learning and its application to antenna modeling and optimization," *IEEE Trans. Ant. Prop.*, vol. 68, no. 5, pp. 3397-3409, 2020.

[30] J. W. Bandler, R. M. Biernacki, S. H. Chen, P. A. Grobelny, and R. H. Hemmers, "Space mapping technique for electromagnetic optimization," *IEEE Trans. Microwave Theory Techn.*, vol. 42, no. 12, pp. 2536-2544, 1994.

[31] S. Tu, Q. S. Cheng, Y. Zhang, J. W. Bandler, and N. K. Nikolova, "Space mapping optimization of handset antennas exploiting thin-wire models," *IEEE Trans. Antennas Propag.*, vol. 61, no. 7, pp. 3797-3807, 2013.

[32] I. A. Baratta, C. B. de Andrade, R. R. de Assis, and E. J. Silva, "Infinitesimal dipole model using space mapping optimization for antenna placement," *IEEE Ant. Wireless Propag. Lett.*, vol. 17, no. 1, pp. 17-20, 2018.

[33] J. Gong, F. Gillon, J. T. Canh, and Y. Xu, "Proposal of a kriging output space mapping technique for electromagnetic design optimization," *IEEE Trans. Magn.*, vol. 53, no. 6, pp. 1-4, 2017.

[34] Y. Su, J. Lin, Z. Fan, and R. Chen, "Shaping optimization of double reflector antenna based on manifold mapping," *Int. Applied Computational Electromagnetic Society Symp. (ACES)*, pp. 1-2, 2017.

[35] S. Koziel and S. D. Unnsteinsson "Expedited design closure of antennas by means of trust-region-based adaptive response scaling," *IEEE Antennas Wireless Prop. Lett.*, vol. 17, no. 6, pp. 1099-1103, 2018.

[36] S. Koziel and L. Leifsson, *Simulation-driven design by knowledge-based response correction techniques*, Springer, New York, 2016.

[37] A. K. Hassan, A. S. Etman, and E. A. Soliman, "Optimization of a novel nano antenna with two radiation modes using kriging surrogate models," *IEEE Photonics Journal*, vol. 10, no. 4, paper no. 4800807, 2018.

[38] J. P. Jacobs, "Characterisation by Gaussian processes of finite substrate size effects on gain patterns of microstrip antennas," *IET Microwaves Ant. Prop.*, vol. 10, no. 11, pp. 1189-1195, 2016.

[39] J. Tak, A. Kantemur, Y. Sharma, and H. Xin, "A 3-D-printed W-band slotted waveguide array antenna optimized using machine learning," *IEEE Ant. Wireless Prop. Lett.*, vol. 17, no. 11, pp. 2008–2012, 2018.

[40] J. Dong, W. Qin, and M. Wang, "Fast multi-objective optimization of multi-parameter antenna structures based on improved BPNN surrogate model," *IEEE Access*, vol. 7, pp. 77692-77701, 2019.

[41] M. B. Jamshidi, A. Lalbakhsh, S. Lotfi, H. Siahkamari, B. Mohamadzade, and J. Jalilian, "A neuro-based approach to designing a Wilkinson power divider," *Int. J. RF Microw. Comput. Aided Eng.*, vol. 30, article no. e22091, 2019.

[42] M. B. Jamshidi, A. Lalbakhsh, B. Mohamadzade, H. Siahkamari, and S. M. H. Mousavi, "A novel neural-based approach for design of microstrip filters," *AEU Int. J. Electr. Comm.*, vol. 110, article no. 152847, 2019.

[43] A. I. J. Forrester and A. J. Keane, "Recent advances in surrogate-based optimization," *Prog. Aerospace Sc.*, vol. 45, pp. 50-79, 2009.

[44] J. A. Easum, J. Nagar, and D. H. Werner, ''Multi-objective surrogate-assisted optimization applied to patch antenna design,'' in *Proc. IEEE Int. Symp. Antennas Propag. USNC/URSI Nat. Radio Sci. Meeting*, San Diego, CA, USA, Jul. 2017, pp. 339-340

[45] S. Mishra, R. N. Yadav, and R. P. Singh, "Directivity estimations for short dipole antenna arrays using radial basis function neural networks," *IEEE Ant. Wireless Prop. Lett.*, vol. 14, pp. 1219-1222, 2015.

[46] T. N. Kapetanakis, I. O. Vardiambasis, M. P. Ioannidou, and A. Maras, "Neural network modeling for the solution of the inverse loop antenna radiation problem," *IEEE Trans. Ant. Propag.*, vol. 66, no. 11, pp. 6283-6290, 2018.

[47] S. Koziel, "Fast simulation-driven antenna design using response-feature surrogates," *Int. J. RF & Microwave CAE*, vol. 25, no. 5, pp. 394-402, 2015.

[48] S. Koziel and A. Pietrenko-Dabrowska, "Design-oriented computationally-efficient feature-based surrogate modelling of multi-band antennas with nested kriging," *AEU Int. J. Electronics Comm.*, vol. 120, 2020.

[49] S. Koziel and A. Pietrenko-Dabrowska, "Expedited feature-based quasi-global optimization of multi-band antennas with Jacobian variability tracking," *IEEE Access*, vol. 8, pp. 83907-83915, 2020.

[50] F. Feng, C. Zhang, W. Na, J. Zhang, W. Zhang, and Q. J. Zhang, "Adaptive feature zero assisted surrogate-based EM optimization for microwave filter design," *IEEE Microwave Wireless Comp. Lett.*, vol. 29, no. 1, pp. 2-4, 2019.

[51] O. Glubokov, and S. Koziel, "EM-driven tuning of substrate integrated waveguide filters exploiting feature-space surrogates," *IEEE Int. Microwave Symp.*, 2014.

[52] S. Koziel and A. Bekasiewicz, "Low-cost surrogate-assisted statistical analysis of miniaturized microstrip couplers," *J. Electromagnetic Waves Appl.*, vol. 30, no. 10, pp. 1345-1353, 2016.

[53] C. Zhang, F. Feng, V. M. R. Gongal-Reddy, Q. J. Zhang, and J. W. Bandler, "Cognition-driven formulation of space mapping for equal-ripple optimization of microwave filters," *IEEE Trans. Microw. Theory Techn.*, vol. 63, no. 7, pp. 2154-2165, 2015.

[54] S. Koziel and J. W. Bandler, "Rapid yield estimation and optimization of microwave structures exploiting feature-based statistical analysis," *IEEE Trans. Microwave Theory Tech.*, vol. 63, no., 1, pp. 107-114, 2015.

[55] S. Koziel and A. Bekasiewicz, "Expedited simulation-driven design optimization of UWB antennas by means of response features," *Int. J. RF and Microwave CAE*, vol. 27, no. 6, paper no. e21102, 2017.

[56] A. R. Conn, N. I. M. Gould, and P. L. Toint, *Trust Region Methods*, MPS-SIAM Series on Optimization, SIAM, Philadelphia, PA, 2000.

[57] A. R. Conn, K. Scheinberg, and L. N. Vicente, *Introduction to Derivative-Free Optimization*, MPS-SIAM Series on Optimization, SIAM, Philadelphia, PA, 2009.

[58] S. Koziel, "Computationally efficient multi-fidelity multi-grid design optimization of microwave structures," *Applied Comput. Electromagn. Society J.*, vol. 25, pp. 578-586, 2010.

[59] N. Jin and Y. Rahmat-Samii, "Advances in particle swarm optimization for antenna designs: Real-number, binary, single-objective and multiobjective implementations," *IEEE Trans. Ant. Propag.*, vol. 55, no. 3, pp. 556-567, 2007.
[60] S. Koziel and A. Pietrenko-Dabrowska, "Performance-based nested surrogate modeling of antenna input characteristics," *IEEE Trans. Ant. Prop.*, vol. 67, no. 5, pp. 2904-2912, 2019.
[61] S. Koziel and A. Bekasiewicz, "Fast re-design and geometry scaling of multi-band antennas using inverse surrogate modeling techniques," *Int. J. Num. Model.*, vol. 31, no. 3, pp. 1-11, 2018.
[62] A. Bekasiewicz and S. Koziel, "Precise control of reflection response in bandwidth-enhanced planar antennas," *Int. J. RF Microwave CAE*, vol. 26, no. 8, pp. 653-659, 2016.
[63] S. Koziel and A. Pietrenko-Dabrowska, "Reduced-cost design closure of antennas by means of gradient search with restricted sensitivity updates", *Metrology Meas. Systems*, vol. 26, no. 4, pp. 595-605, 2019
[64] C. Sim, M. Chang, and B. Chen, "Microstrip-fed ring slot antenna design with wideband harmonic suppression," *IEEE Trans. Ant. Propag.*, vol. 62, no. 9, pp. 4828-4832, 2014.
[65] M. G. N. Alsath and M. Kanagasabai, "Compact UWB monopole antenna for automotive communications," *IEEE Trans. Ant. Prop.*, vol. 63, no. 9, pp. 4204-4208, 2015.
[66] D. R. Prado, J. A. López-Fernández, M. Arrebola, and G. Goussetis, "Support vector regression to accelerate design and crosspolar optimization of shaped-beam reflectarray antennas for space applications," *IEEE Trans. Antennas Propag.*, vol. 67, no. 3, pp. 1659-1668, 2019.
[67] B. Liu, M. O. Akinsolu, N. Ali, and R. Abd-Alhameed, "Efficient global optimisation of microwave antennas based on a parallel surrogate model-assisted evolutionary algorithm," *IET Microw. Antennas Propag.*, vol. 13, no. 2, pp. 149-155, 2019.
[68] M. O. Akinsolu, B. Liu, V. Grout, P. I. Lazaridis, M. E. Mognaschi, and P. D. Barba, "A parallel surrogate model assisted evolutionary algorithm for electromagnetic design optimization," *IEEE Trans. Emerging Topics Comput. Intell.*, vol. 3, no. 2, pp. 93-105, 2019.
[69] Y. Sharma, H. H. Zhang, and H. Xin, "Machine learning techniques for optimizing design of double T-shaped monopole antenna," *IEEE Trans. Antennas Propag.*, vol. 68, no. 7, pp. 5658-5663, 2020.
[70] Q. Wu, H. Wang, and W. Hong, "Multistage collaborative machine learning and its application to antenna modeling and optimization," *IEEE Trans. Ant. Propag.*, vol. 68, no. 5, pp. 3397-3409, 2020.

ANNA PIETRENKO-DABROWSKA received the M.Sc. and Ph.D. degrees in electronic engineering from Gdansk University of Technology, Poland, in 1998 and 2007, respectively. Currently, she is an Associate Professor with Gdansk University of Technology, Poland. Her research interests include simulation-driven design, design optimization, control theory, modeling of microwave and antenna structures, numerical analysis.

SLAWOMIR KOZIEL received the M.Sc. and Ph.D. degrees in electronic engineering from Gdansk University of Technology, Poland, in 1995 and 2000, respectively. He also received the M.Sc. degrees in theoretical physics and in mathematics, in 2000 and 2002, respectively, as well as the PhD in mathematics in 2003, from the University of Gdansk, Poland. He is currently a Professor with the Department of Engineering, Reykjavik University, Iceland. His research interests include CAD and modeling of microwave and antenna structures, simulation-driven design, surrogate-based optimization, space mapping, circuit theory, analog signal processing, evolutionary computation and numerical analysis.